PPRIME FORUM

« Mechanical Design and Mechatronics of robotics systems »

Futuroscope, November , 2014

Lecture hall, SP2MI building

rue Gustave Eiffel Futuroscope Chasseneuil, France

*_*_*

The FORUM organized by the Pprime Institute offers the opportunity to PhD students and researchers from the robotics community to meet experts in order to exchange with them about most recent scientific results. This event provides to participants a space of reflection and privileged exchange.

The FORUM is dedicated to Mechanical Design and Mechatronics of robotics systems. Two themes, in the field of interest of the robotics team of Pprime institute, are considered during this FORUM.

- The design of mechanical hands for dexterous manipulation,
- The design of complex poly-articulated mechanisms (parallel mechanisms).

The forum is organized over three days with a program focused on presentations and panel discussions. In this context, we will have four guest speakers:

- Yukio Takeda, Professor, Tokyo Institute of Technology, Japan
- Philippe Wenger, Directeur de recherches au CNRS, IRCCyN-Nantes, France
- Markus Grebenstein, doctor, DLR German Aerospace Center, Munich, Germany
- Chin-Hsing Kuo, Professor, National Taiwan University of Science and Technology, Taiwan

PPRIME Forum

«Mechanical Design and Mechatronics of robotics systems»

Thursday, November 6: « Kinematic optimization of complex poly-articulated systems »

Morning: 10h-12h

- Yukio Takeda, Professor Tokyo Institute of Technology - Japon
  - Title : « Kinematic Design of Compensatable Parallel Manipulators »
  - Panel discussion

Afternoon: 14h-17h

- Philippe Wenger, Directeur de recherches au CNRS IRCCyN Nantes - France.
  - Title : « Coping with singularities in the design of parallel-manipulators »
  - Panel discussion
- Yukio Takeda, Professor Tokyo Institute of Technology – Japon
  - Title : « Kinematic and Dynamic Analysis and Design of 3-RPSR Parallel Mechanism for Pipe-Bender »
  - Panel Discussion

Friday, November 19: « Design of medical robots / Design of mechanical hands »

Morning: 10h-12h

- Chin-Hsing Kuo, Professor National Taiwan University of Science and Technology - Taiwan
  - Title : « Applications of Mechanism Design Theories for Surgical Robotics »
  - Panel Discussion

Afternoon: 14h-17h

- Sebastian Wolf, Doctor, DLR German Aerospace Center, Munich, Germany
  - Title : « Design of the DLR-Hand Arm System - Focus on Variable Impedance Actuation (VIA) »
  - Panel Discussion

Kinematic and Dynamic Analysis and Design of 3-RPSR Parallel Mechanism for Pipe-Bender

Yukio Takeda, Dr. Eng.

Professor, Dept .of Mechanical Sciences and Engineering

Director, Super-Mechano System Innovation & Development Center

Tokyo Institute of Technology, Japan

http://www.mech.titech.ac.jp/~msd/, http://www.sms.titech.ac.jp/

Email: takeda@mech.titech.ac.jp

Presented at Robotics PPRIME Forum 2014, November 6, 2014, University of Poitiers, France

Table of contents

Demand for pipes of 3D shape

Tokyo Institute of Technology
Mechanical Systems Design Lab.

Support devices to
reduce tremor effect

Objects with a three-dimensional shape obtained by bending a straight pipe with a uniform cross section are being used as components in many applications because they contribute to mass reduction, rigidity improvement, cost reduction, design improvement.

Demand for pipes of 3D shape

Tokyo Institute of Technology
Mechanical Systems Design Lab.

Support devices to
reduce tremor effect

Mass production system is not appropriate for manufacturing components for welfare devices.
Tailor-made manufacturing for fitting to each person is necessary.

Objects with a three-dimensional shape obtained by bending a straight pipe with a uniform cross section are being used as components in many applications because they contribute to mass reduction, rigidity improvement, cost reduction, design improvement.

Penetration bending method

Tokyo Institute of Technology
Mechanical Systems Design Lab.

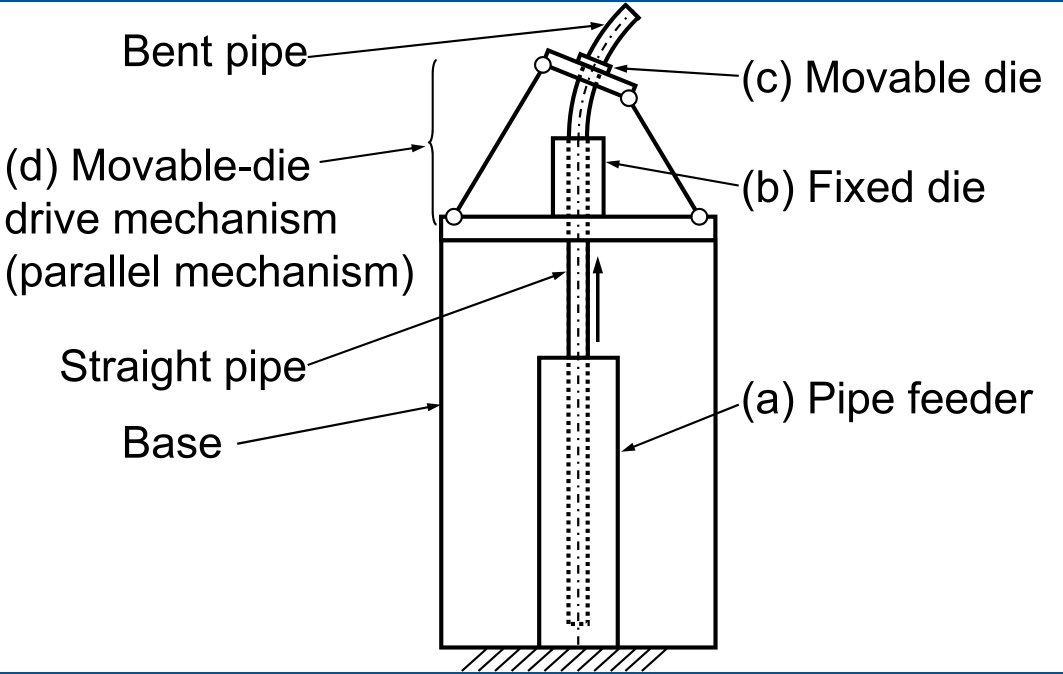

Configuration of pipe bender using parallel mechanism based on the penetration bending method

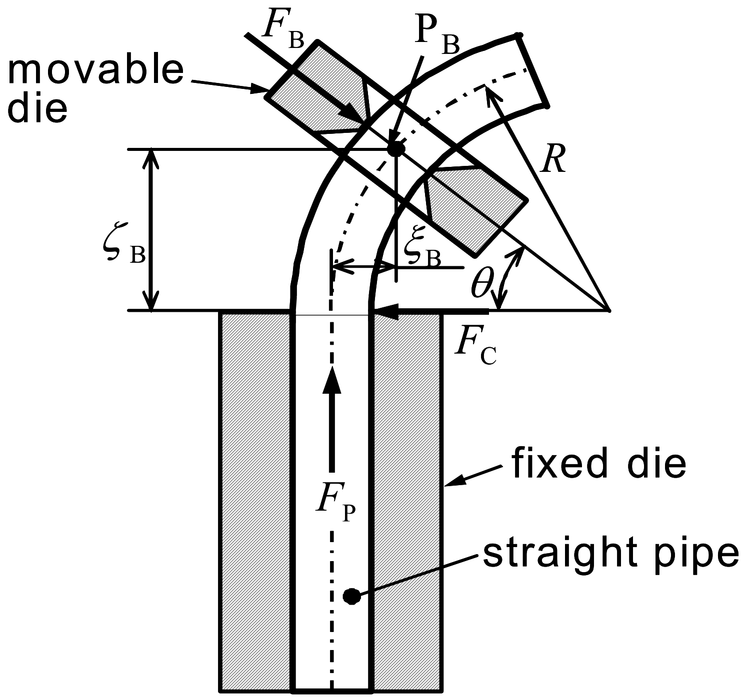

Geometrical parameters and forces applied to the pipe

FEM analysis demo

The penetration bending method is one way to manufacture three-dimensional pipes. A straight pipe is bent by pushing it through a fixed die and movable die, which is in an offset position. The cross sections of both dies have a shape counter to that of the pipe. The position and orientation of the movable die at every period are controlled in accordance with the desired shape of the pipe after bending. The motion of the movable die is synchronized with that of the pipe feeder. This method can be used to bend a pipe with an arbitrary cross section by using two simple dies. Expensive dies with three-dimensional shapes corresponding to the external shape of the pipe to be bent are not needed.

Penetration bending method

Tokyo Institute of Technology
Mechanical Systems Design Lab.

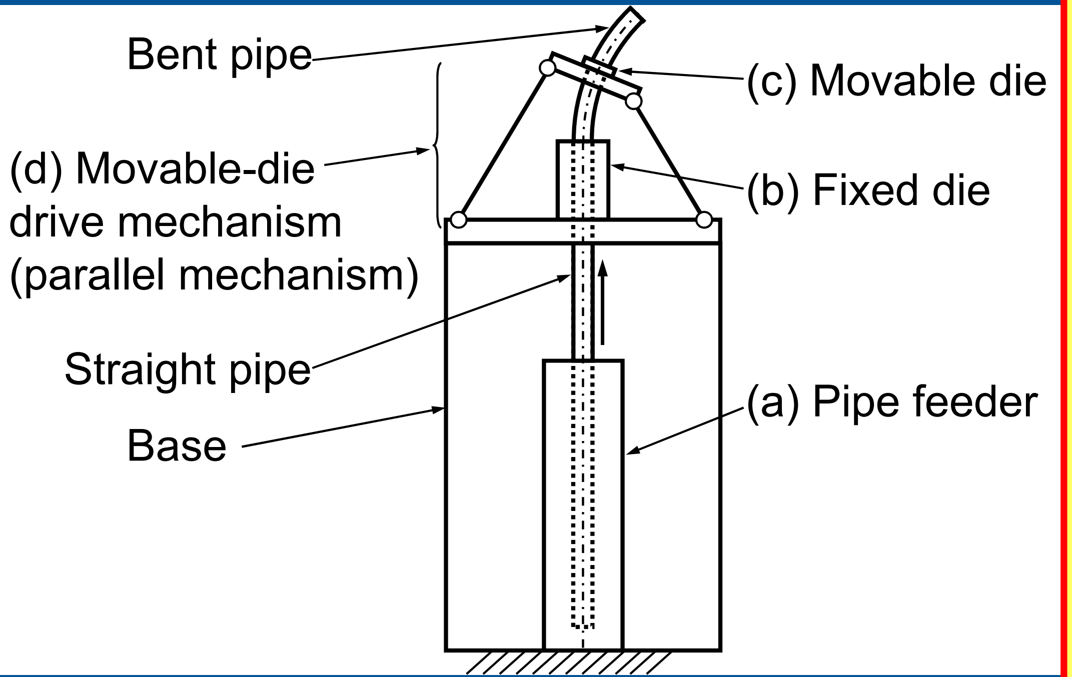

Target of our research:
Movable-die drive mechanism, dominating shape complexity, accuracy and surface quality of the bent pipe.

Parallel mechanism:
Good candidate as the movable-die driving mechanism because of its advantages in accuracy and rigidity.

Configuration of pipe bender using parallel mechanism based on the penetration bending method

FEM analysis demo

The penetration bending method is one way to manufacture three-dimensional pipes. A straight pipe is bent by pushing it through a fixed die and movable die, which is in an offset position. The cross sections of both dies have a shape counter to that of the pipe. The position and orientation of the movable die at every period are controlled in accordance with the desired shape of the pipe after bending. The motion of the movable die is synchronized with that of the pipe feeder. This method can be used to bend a pipe with an arbitrary cross section by using two simple dies. Expensive dies with three-dimensional shapes corresponding to the external shape of the pipe to be bent are not needed.

Pipe bender using parallel mechanism

Photo of the CNC pipe bender using Stewart-Gough platform (Kikuchi Seisakusho Co., Ltd.) (demo1) (demo2)

This CNC pipe bender has been used to manufacture many three-dimensional objects for several years. However, it still has problems bending pipes with a small curvature radius due to its limited orientation capability. Full rotation of the movable die around the axis of the pipe is needed to form pipes with an axis-symmetric shape such as helical. However, parallel mechanisms such as the Stewart-Gough platform can not achieve such motion.

Target of our research

- ✓ Kinematic Design of Movable-Die Drive Mechanism with Orientation Capability which Enables Bending of Pipes with Complex Shapes (Especially with Large Curvature)
  →Proposition of 3-RPSR parallel mechanism and its kinematic design
- ✓ Design of Movable-Die Drive Mechanism with High Stiffness to Achieve Precise Bending
  →Evaluation of the designed mechanism in terms of compliance characteristics in pipe bending
- ✓ Modeling of penetration pipe bending and compensation of springback of pipe and clearance at dies
- ✓ Prototyping
- ✓ Experimental validation

Table of contents

Tokyo Institute of Technology
Mechanical Systems Design Lab.

3-RPSR parallel mechanism as movable-die drive mechanism

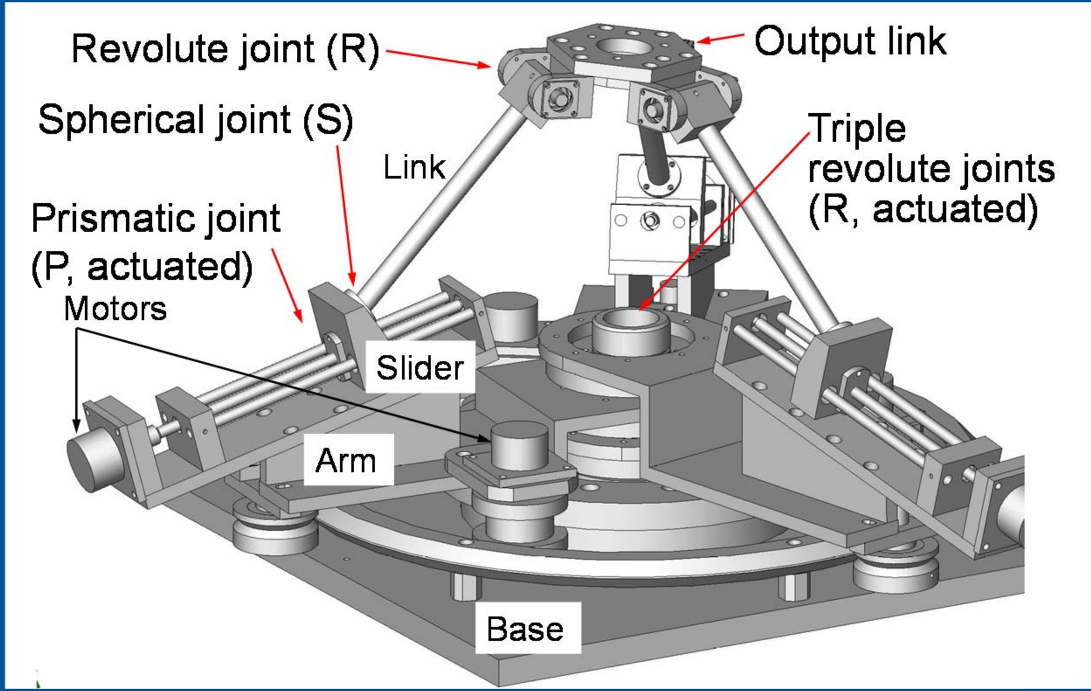

2nd prototype of our pipe bender using 3-RPSR parallel mechanism

Features of our 3-RPSR mechanism:

video

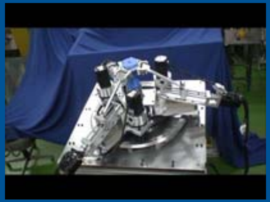

(a) Three connecting chains.
(b) Triple revolute joints.
(c) Revolute joint on the output link
(d) Appropriate slider angle

Full rotation and large inclination of the output link are achieved.

Tokyo Institute of Technology
Mechanical Systems Design Lab.

Pipe bender using 3-RPSR parallel mechanism

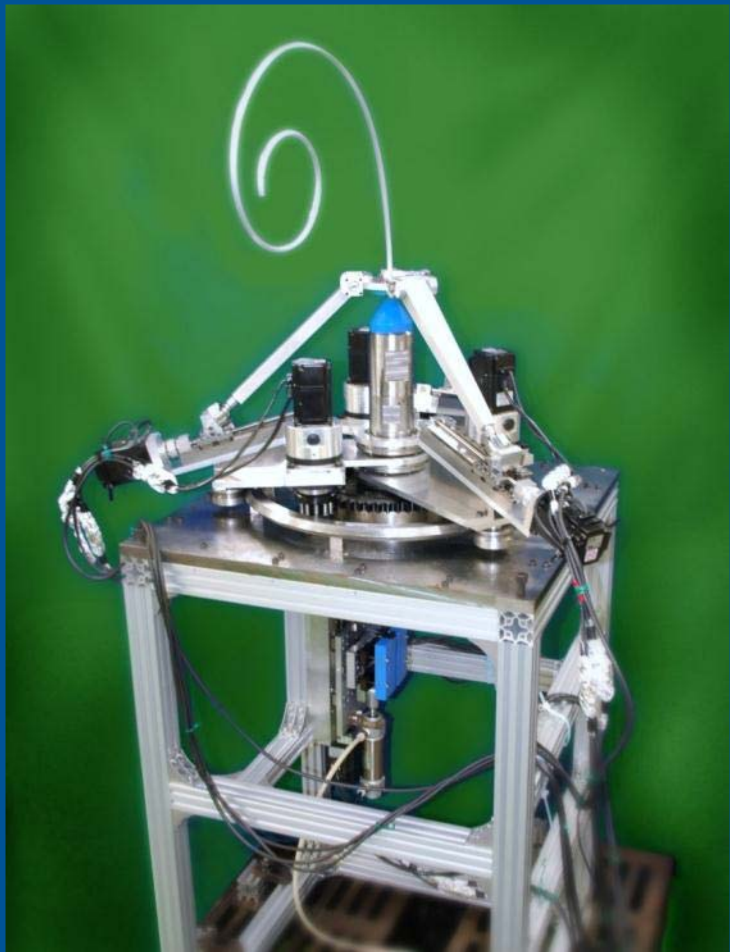

Clothoid curve

Uniform helix

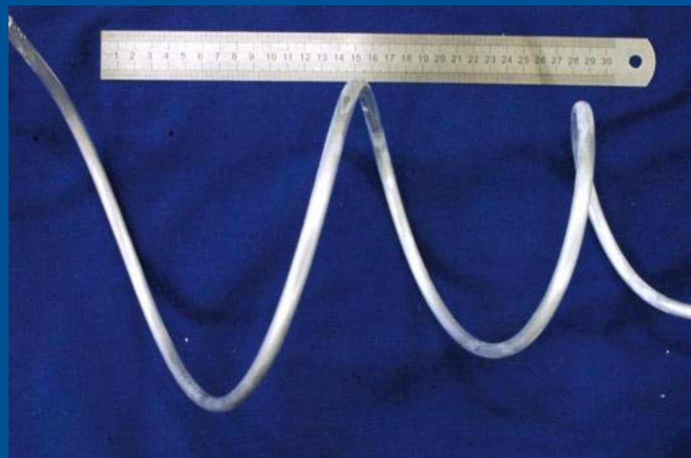

Non-uniform helix

Bent pipes by our 2nd prototype pipe bender

Demand

Demand:
Our prototype pipe bender using a 3-RPSR parallel mechanism as the movable-die drive mechanism successfully achieved manufacturing of three dimensional shaped pipes such as clothoid curves, uniform helix and non-uniform helix. Manufacturing more complex shaped pipes are required. However, we found that design of mechanism for achieving better orientation capability is required to the movable-die drive mechanism for this purpose.

Collision of movable and fixed dies

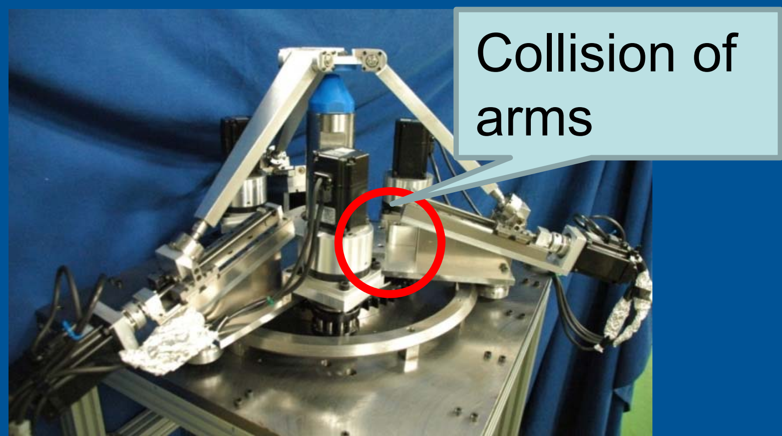

Collision of arms

Demand for new design

Demand:
Our prototype pipe bender using a 3-RPSR parallel mechanism as the movable-die drive mechanism successfully achieved manufacturing of three dimensional shaped pipes such as clothoid curves, uniform helix and non-uniform helix. However, we found that better orientation capability is required to the movable-die drive mechanism for manufacturing complex three-dimensional shaped pipes.

Purpose:
The purpose of this research is to clarify the relationship between kinematic parameters and orientation capability of 3-RPSR parallel mechanism. Better mechanical design is also investigated to extend the motion range of the arms. Then, a mechanism having a better orientation capability is clarified.

Description of the mechanism

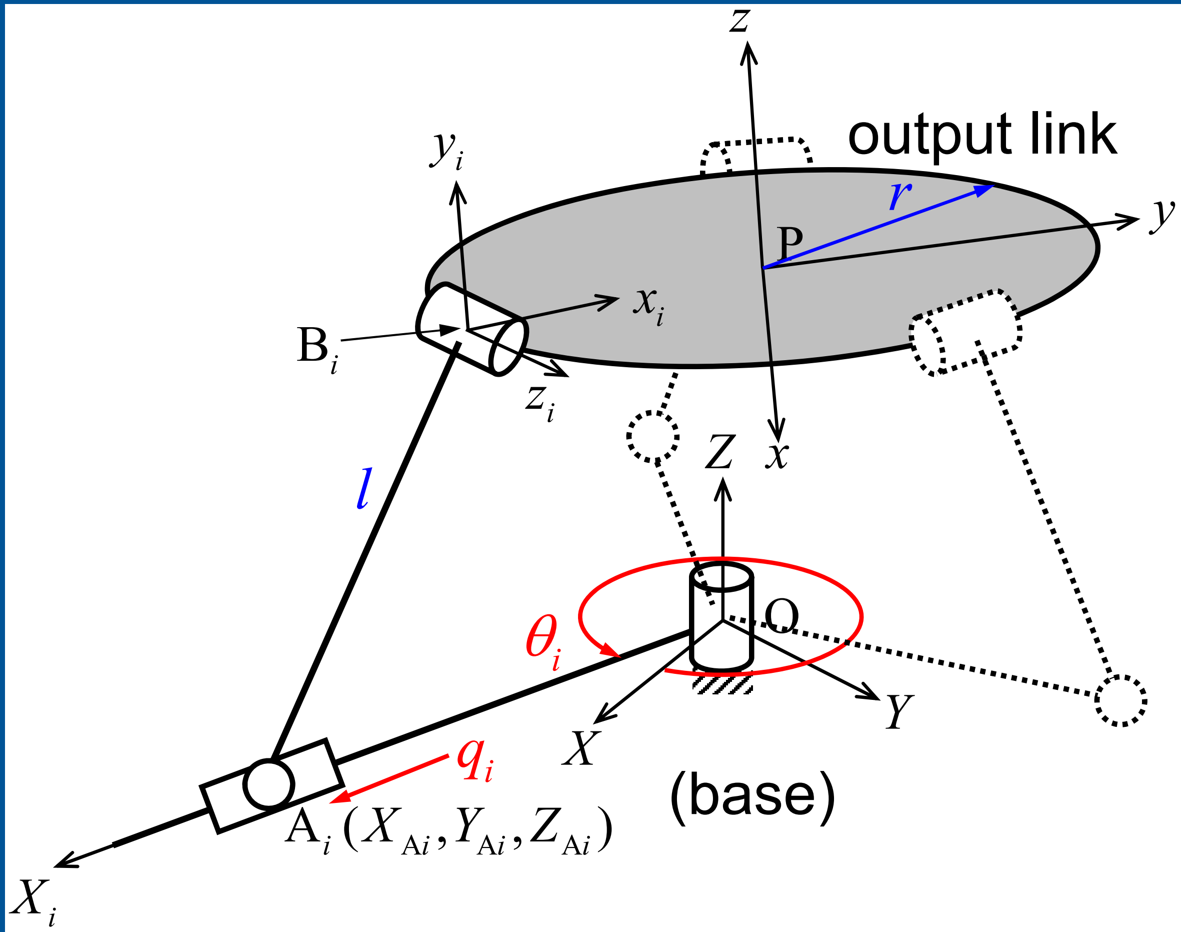

Definition of kinematic constants

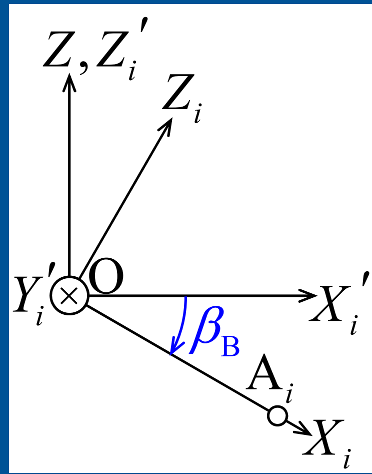

Definition of angle β_B

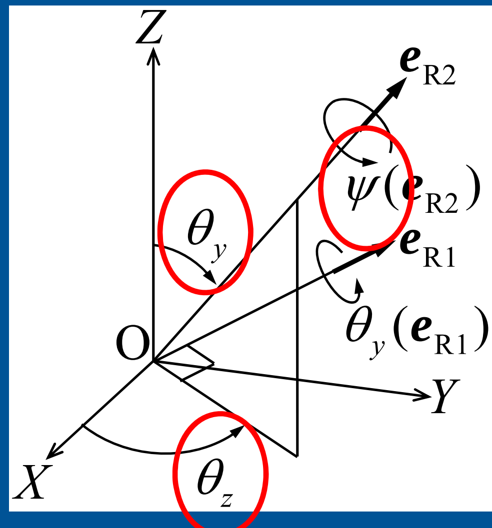

Definition of orientation angles

Predominant factors of orientation capability

1. Singular configurations
2. Required swing angle of the spherical joint
3. Closest angle between neighboring arms

Kinematic parameters will be optimized.

Mechanical design will be improved.

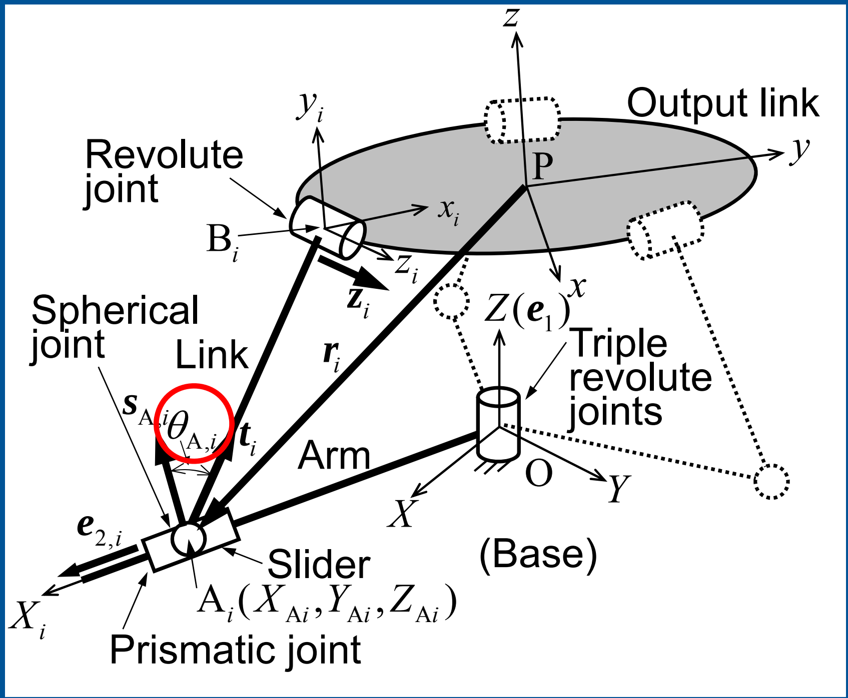

3-RPSR mechanism

Photo of spherical joint

Analysis of orientation capability

Considered points:

(1)Maximum inclination angle of movable die (θ_y)
(2)Maximum swing angle of spherical joint (θ_A)

Target motion: (typical motion for bending helical pipes)

$$X_P = X''\cos\theta_z, Y_P = X''\sin\theta_z, Z_P = Z_O - S_Z + 2\frac{S_Z}{S_X}X'', \theta_y = \frac{\theta_{y,\max}}{S_X}X''$$

$$\psi = 0, \theta_z = (i-1)\pi/9 (i=1,\cdots,6),\ X'':[-S_X, S_X]$$

$\theta_{y,\max}$: maximum inclination angle,
S_X, S_Z: maximum strokes in XZ plane

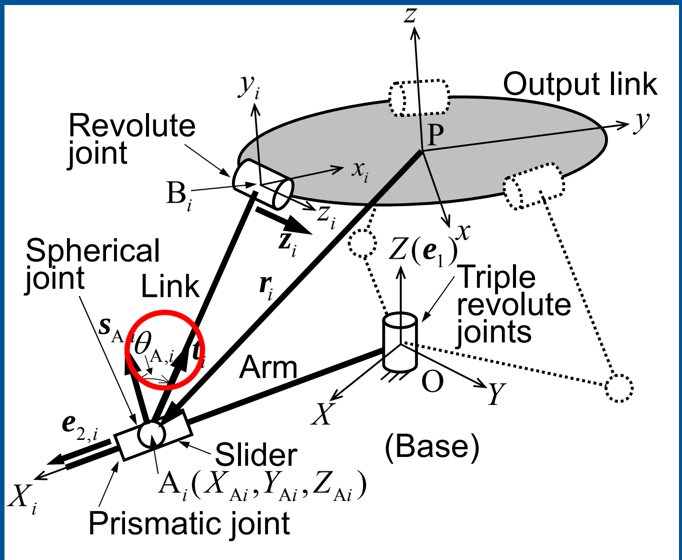

3-RPSR mechanism

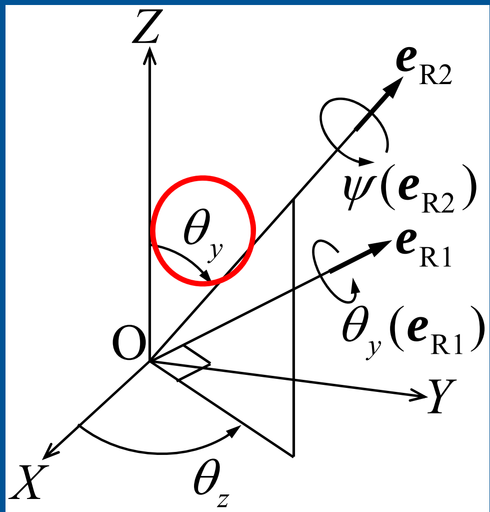

Definition of orientation angles

Analysis of orientation capability

Considered points:

(1)Maximum inclination angle of movable die (θ_y)
(2)Maximum swing angle of spherical joint (θ_A)

Target motion: (typical motion for bending helical pipes)

$$X_P = X''\cos\theta_z, Y_P = X''\sin\theta_z, Z_P = Z_O - S_Z + 2\frac{S_Z}{S_X}X'', \theta_y = \frac{\theta_{y,\max}}{S_X}X''$$

$$\psi = 0, \theta_z = (i-1)\pi/9 (i = 1,\cdots,6),\ X'':[-S_X, S_X]$$

$\left\{ \begin{array}{l} \theta_{y,\max}\text{: maximum inclination angle,} \\ S_X, S_Z\text{: maximum strokes in XZ plane} \end{array} \right\}$

The maximum inclination angle of the movable die and the maximum swing angle of spherical joint are dependent on the direction of the inclination. So, considering several θ_z, maximization of the maximum and minimum of the maximum inclination angle and minimization of the required maximum swing angle of spherical joint were considered.

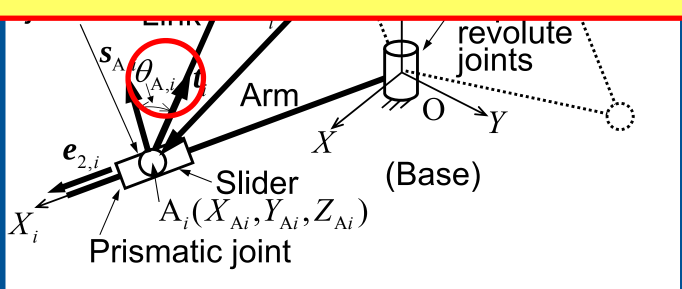

3-RPSR mechanism

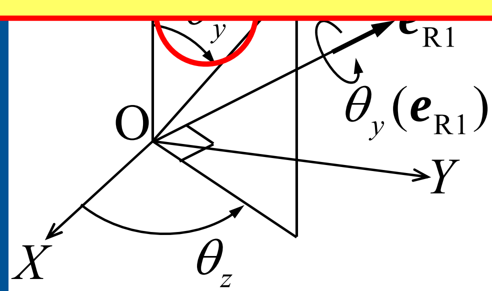

Definition of orientation angles

Analysis of orientation capability

Tokyo Institute of Technology
Mechanical Systems Design Lab.

Evaluation indices:

(1-1) Maximum of the maximum inclination angles at a constant θ_z :
$\max(\theta_{y,1}(\theta_z\text{=cost.}))$

(1-2) Minimum of the maximum inclination angles at a constant θ_z :
$\min(\theta_{y,1}(\theta_z\text{=cost.}))$

(2) Ratio of the maximum swing angle of spherical joint at $\max(\theta_{y,1}(\theta_z\text{=cost.}))$ to $\max(\theta_{y,1}(\theta_z\text{=cost.}))$: $\theta_{A,\max}/\max(\theta_{y,1}(\theta_z\text{=cost.}))$

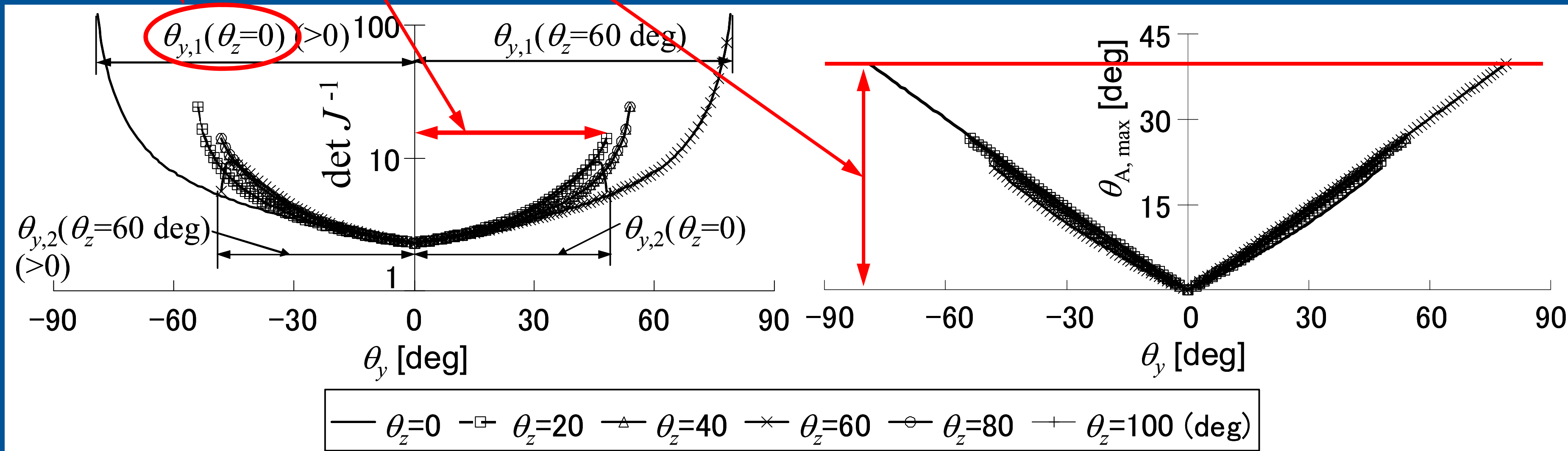

Change of det J^{-1} and $\theta_{A,\max}$ with respect to θ_y (r=45 mm, l=150 mm, β_B=0, S_X=S_Z=16 mm)

Analysis of orientation capability

Evaluation indices:

(1-1) Maximum of the maximum inclination angles at a constant θ_z :
$\max(\theta_{y,1}(\theta_z\text{=cost.}))$

(1-2) Minimum of the maximum inclination angles at a constant θ_z :
$\min(\theta_{y,1}(\theta_z\text{=cost.}))$

(2) Ratio of the maximum swing angle of spherical joint at $\max(\theta_{y,1}(\theta_z\text{=cost.}))$ to $\max(\theta_{y,1}(\theta_z\text{=cost.}))$: $\theta_{A,\max}/\max(\theta_{y,1}(\theta_z\text{=cost.}))$

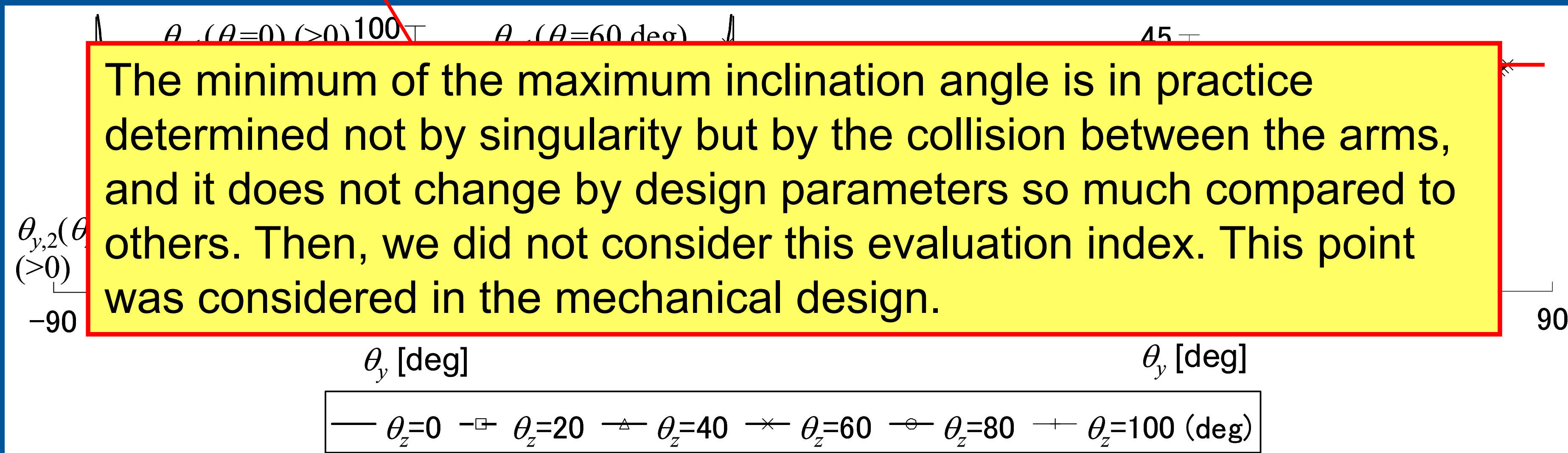

The minimum of the maximum inclination angle is in practice determined not by singularity but by the collision between the arms, and it does not change by design parameters so much compared to others. Then, we did not consider this evaluation index. This point was considered in the mechanical design.

Change of $\det J^{-1}$ and $\theta_{A,\max}$ with respect to θ_y (r=45 mm, l=150 mm, β_B=0, S_X=S_Z=16 mm)

Results (summary)

Tokyo Institute of Technology
Mechanical Systems Design Lab.

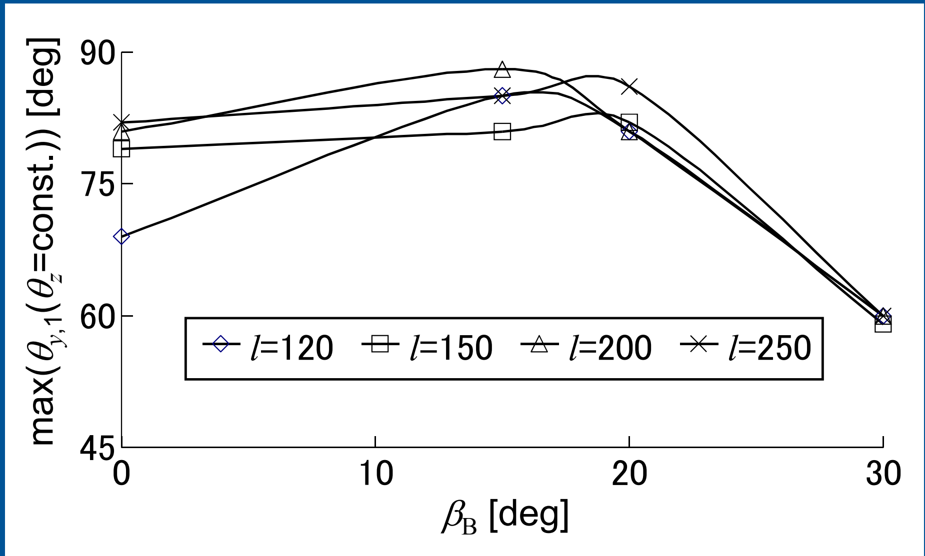

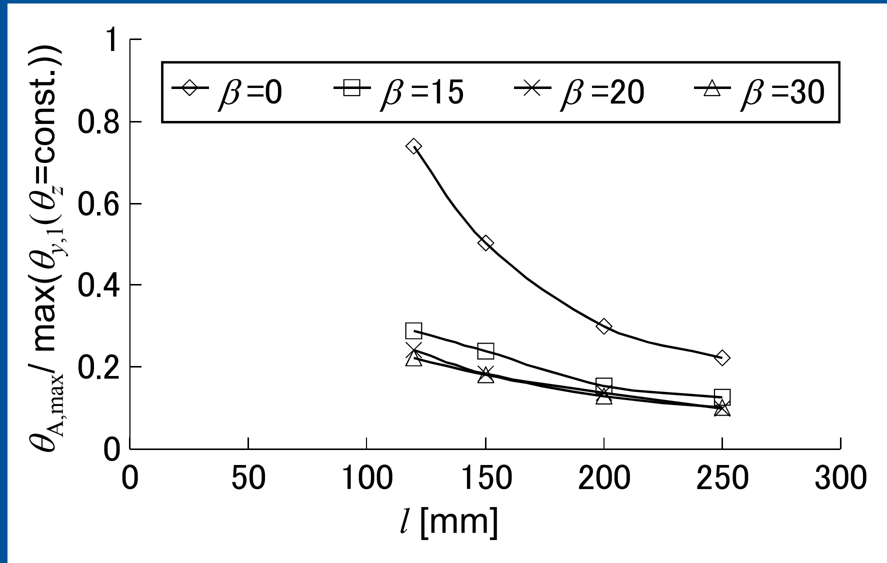

Relationships between design parameters and the evaluation indices in terms of maximum inclination angle and required maximum swing angle of the spherical joint(standard design parameters: r=45 mm, l=150 mm, β_B=15 deg)

Results (summary)

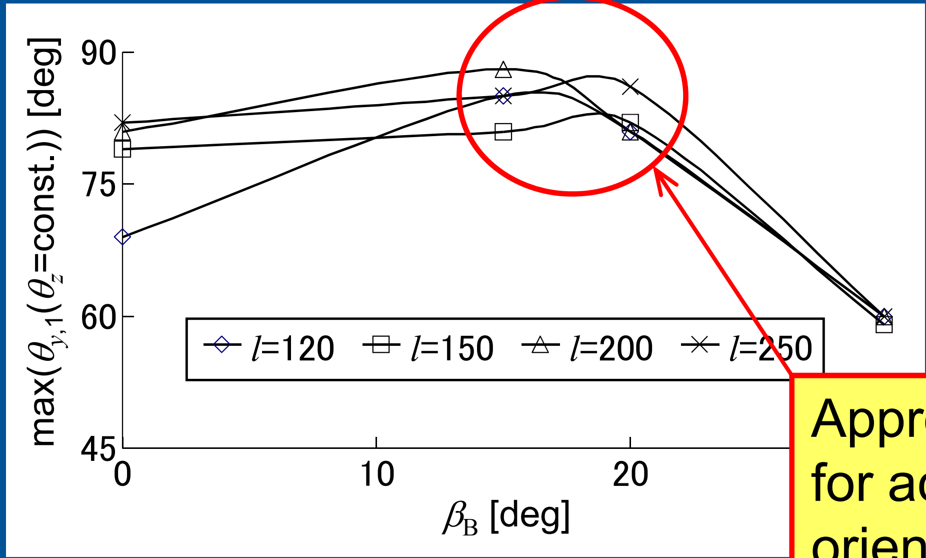

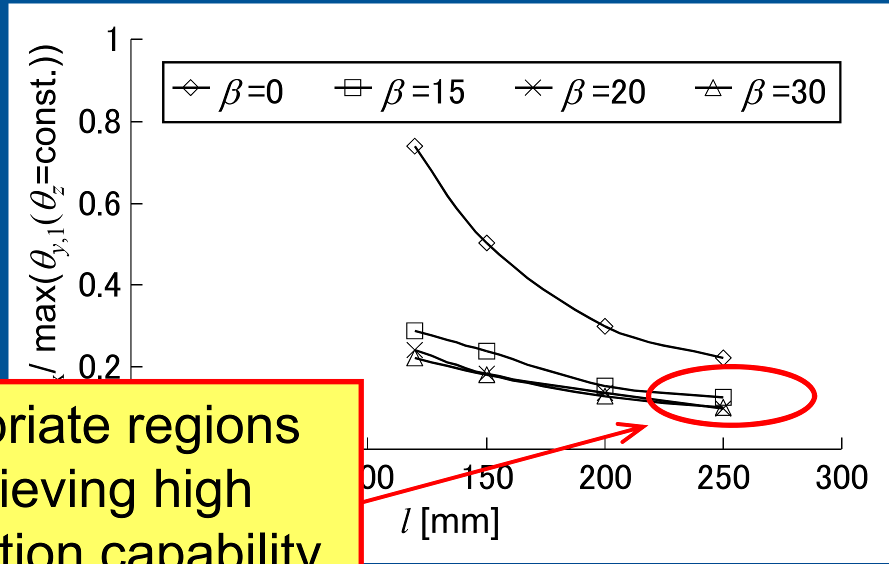

Appropriate regions for achieving high orientation capability

Relationship between design parameters and the evaluation indices in terms of maximum inclination angle and required maximum swing angle of the spherical joint(standard design parameters: r=45 mm, l=150 mm, β_B=15 deg)

Based on the analysis results, we optimized kinematic constants, then we designed a mechanism.

Prototype mechanism

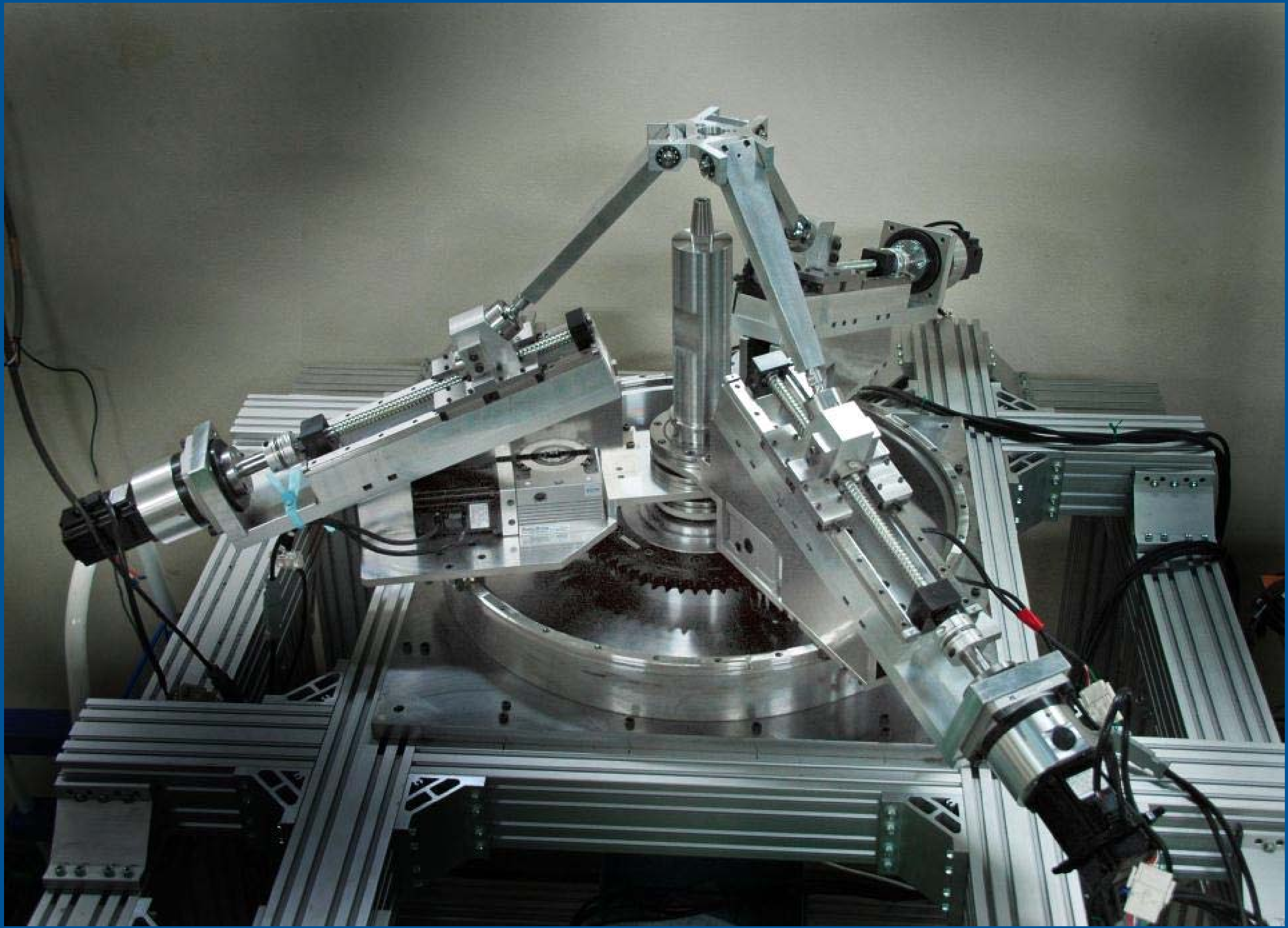

Overview of the prototype

Prototype mechanism

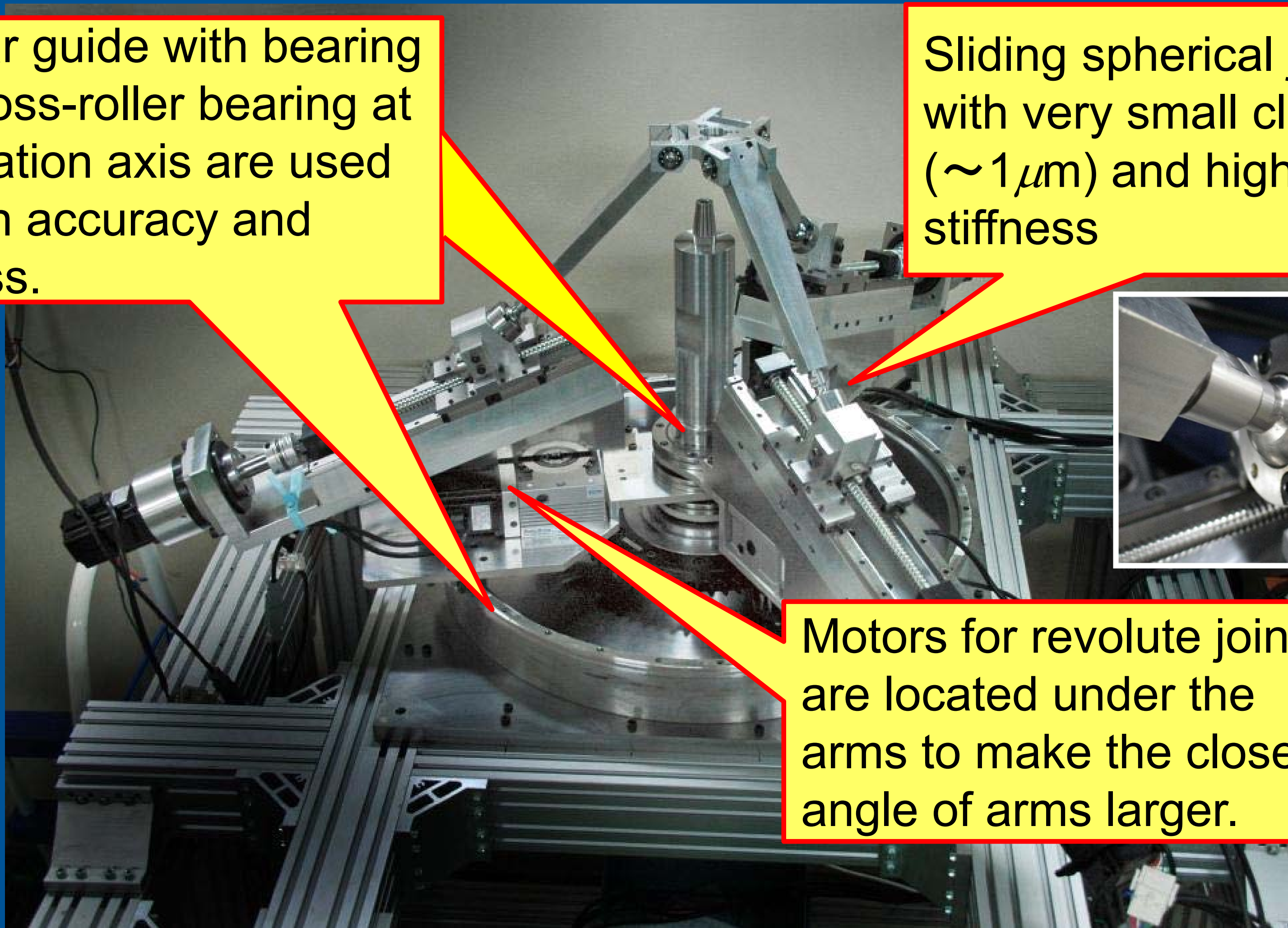


Overview of the prototype

Prototype mechanism

Tokyo Institute of Technology
Mechanical Systems Design Lab.

Map of inclination angle

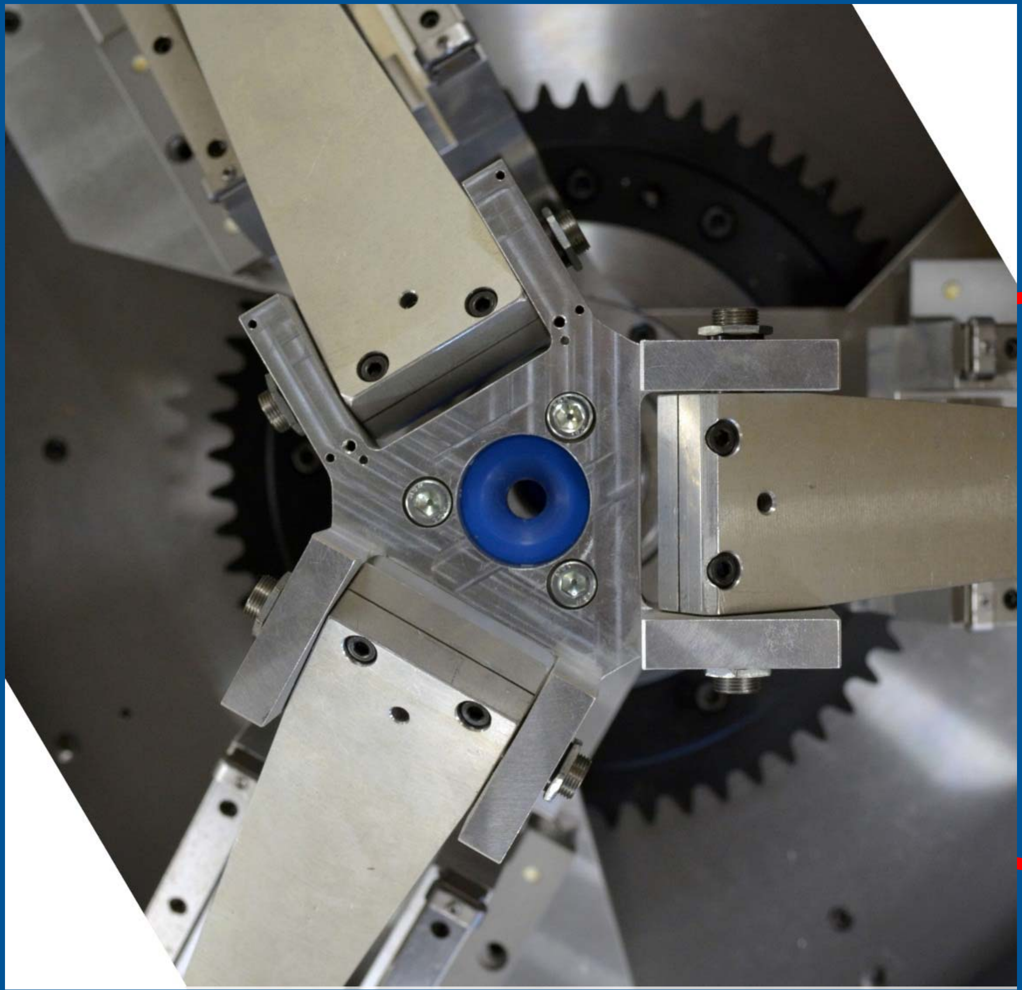

Plot of the limit of Inclination angle in each direction

Min. inclination (39deg)

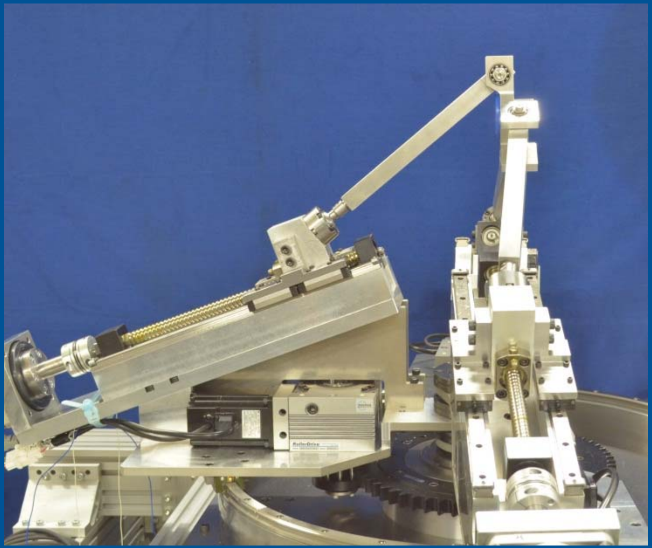

Max. inclination (90deg)

Prototype mechanism

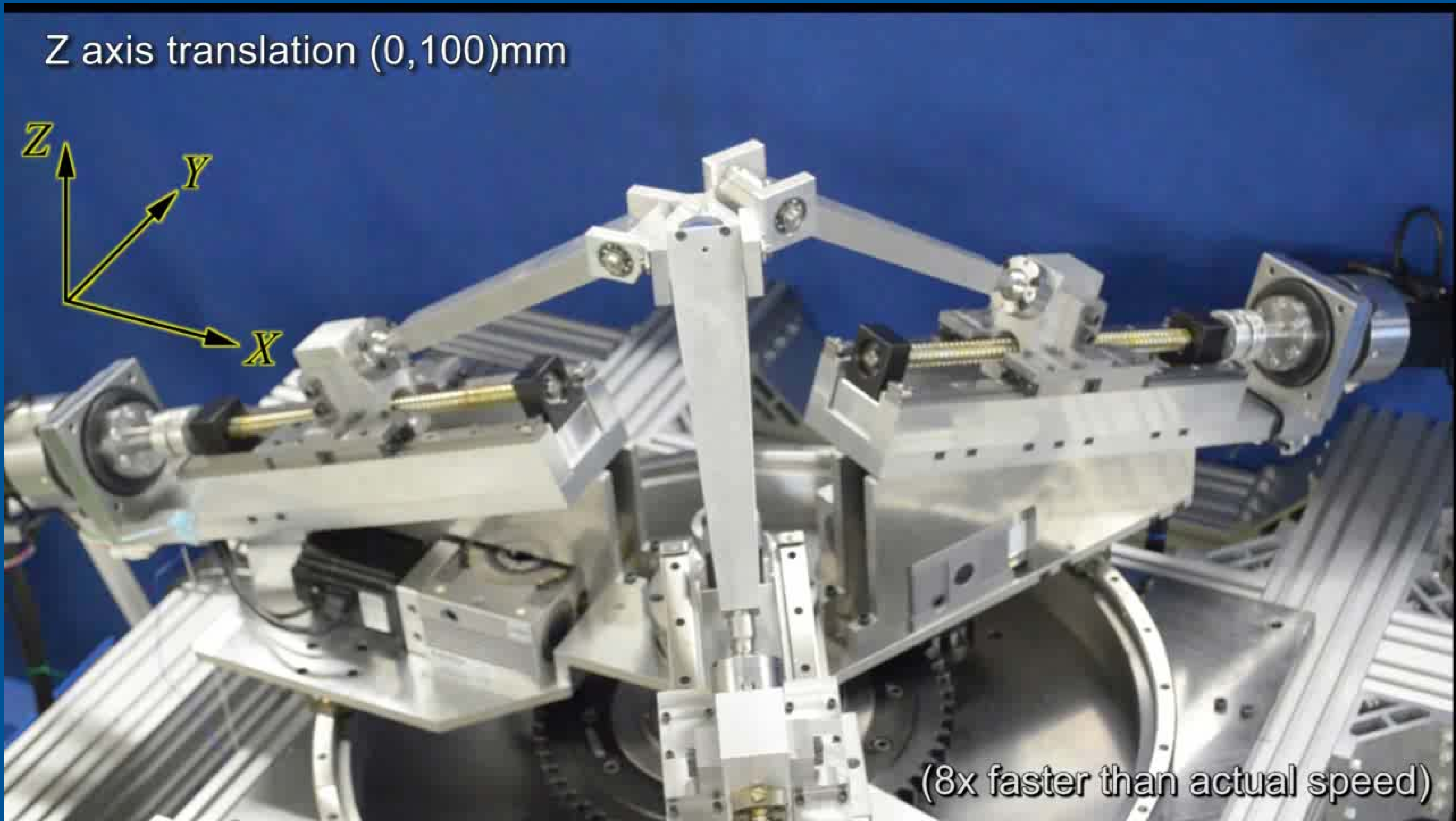

Demonstration video

Summary-Kinematic Design

Kinematic analysis of a 3-RPSR parallel mechanism with six DOF, which has been applied to a movable-die drive mechanism of pipe bender, has been done to clarify the relationship between its design parameters and orientation capability. Based on the results of analysis, a mechanism that can achieve a high orientation capability was designed, and a prototype has been built. Its orientation capability has been revealed, and it has been shown that our prototype mechanism achieved a superior orientation capability.

Table of contents

1. Introduction
2. Kinematic design of 3-RPSR parallel mechanism for movable-die drive mechanism of pipe bender
3. Compliance analysis of 3-RPSR parallel mechanism
4. Compensation of springback effect of pipe and clearance at dies for precise bending
5. Experiments
6. Summary (Conclusions and future works)

Compliance model

Tokyo Institute of Technology
Mechanical Systems Design Lab.

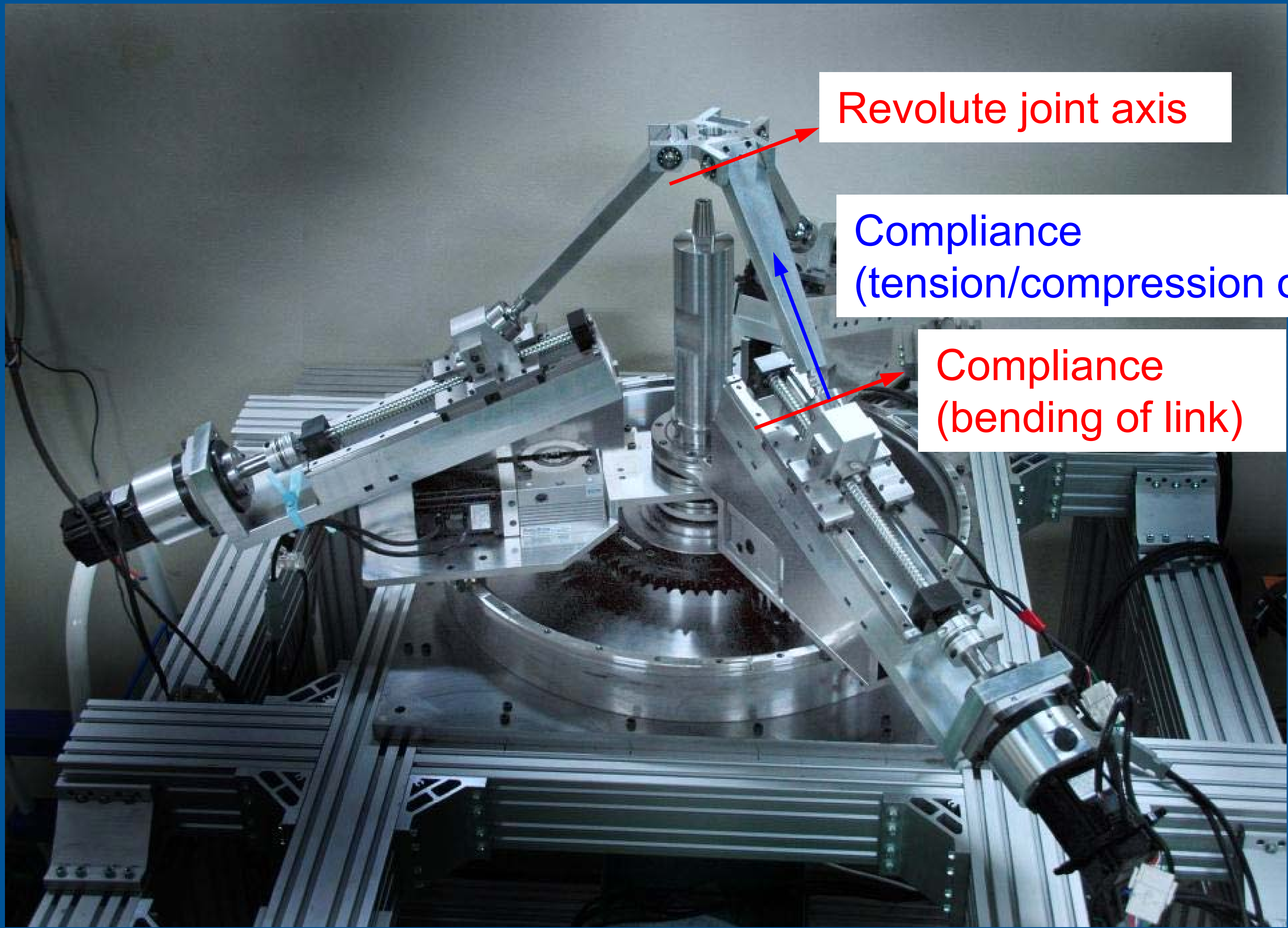

Overview of the prototype

Jacobian matrices

Tokyo Institute of Technology
Mechanical Systems Design Lab.

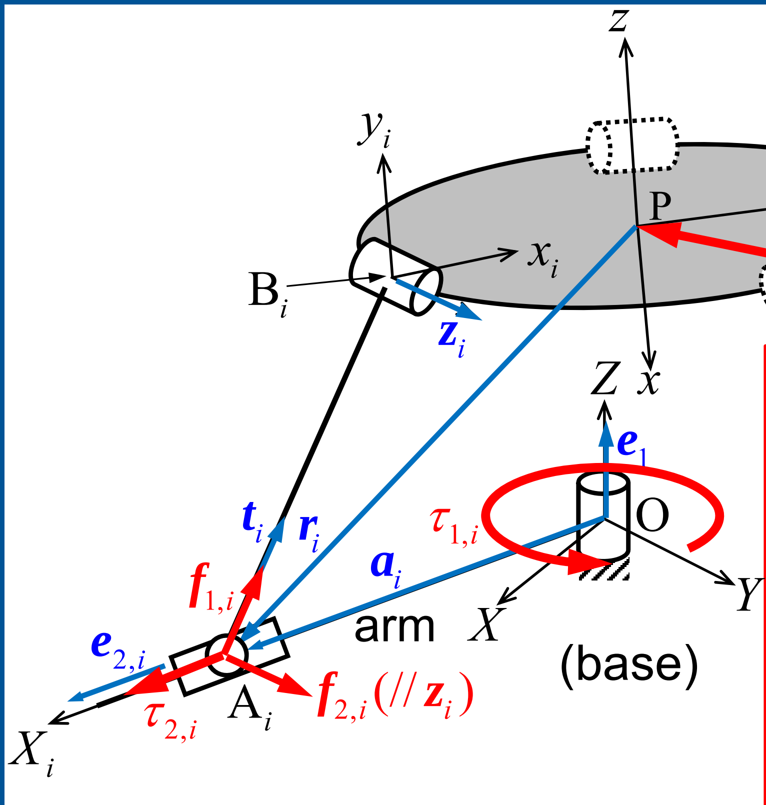

$\tau_{1,i}$: input torque(R)

$\tau_{2,i}$: input force(P)

$\boldsymbol{F}$: external force

$\boldsymbol{M}$: external moment

$f_{1,i}$: joint force

$f_{2,i}$: joint force

External force, input torque/force and joint forces

External force vs. input force/torque:

$$\begin{bmatrix} \boldsymbol{F} \\ \boldsymbol{M} \end{bmatrix} = -J_1 J_2^{-1} \begin{bmatrix} \boldsymbol{\tau}_1 \\ \boldsymbol{\tau}_2 \end{bmatrix} = -J\boldsymbol{\tau}$$

External force vs. joint force at Ai:

$$\begin{bmatrix} \boldsymbol{F} \\ \boldsymbol{M} \end{bmatrix} = -J_1 \boldsymbol{f}$$

Relationship between joint forces and input force/torque:

$$\boldsymbol{\tau} = J_2 \boldsymbol{f}$$

Matrices J_1 and J_2:

$$J_1 = \begin{bmatrix} \boldsymbol{t}_1 & \boldsymbol{t}_2 & \boldsymbol{t}_3 & \boldsymbol{z}_1 & \boldsymbol{z}_2 & \boldsymbol{z}_3 \\ \boldsymbol{r}_1 \times \boldsymbol{t}_1 & \boldsymbol{r}_2 \times \boldsymbol{t}_2 & \boldsymbol{r}_3 \times \boldsymbol{t}_3 & \boldsymbol{r}_1 \times \boldsymbol{z}_1 & \boldsymbol{r}_2 \times \boldsymbol{z}_2 & \boldsymbol{r}_3 \times \boldsymbol{z}_3 \end{bmatrix} \quad J_2 = \begin{bmatrix} \{\boldsymbol{a}_1 \times \boldsymbol{t}_1, \boldsymbol{e}_1\} & 0 & 0 & \{\boldsymbol{a}_1 \times \boldsymbol{z}_1, \boldsymbol{e}_1\} & 0 & 0 \\ 0 & \{\boldsymbol{a}_2 \times \boldsymbol{t}_2, \boldsymbol{e}_1\} & 0 & 0 & \{\boldsymbol{a}_2 \times \boldsymbol{z}_2, \boldsymbol{e}_1\} & 0 \\ 0 & 0 & \{\boldsymbol{a}_3 \times \boldsymbol{t}_3, \boldsymbol{e}_1\} & 0 & 0 & \{\boldsymbol{a}_3 \times \boldsymbol{z}_3, \boldsymbol{e}_1\} \\ \{\boldsymbol{t}_1, \boldsymbol{e}_{2,1}\} & 0 & 0 & \{\boldsymbol{z}_1, \boldsymbol{e}_{2,1}\} & 0 & 0 \\ 0 & \{\boldsymbol{t}_2, \boldsymbol{e}_{2,2}\} & 0 & 0 & \{\boldsymbol{z}_2, \boldsymbol{e}_{2,2}\} & 0 \\ 0 & 0 & \{\boldsymbol{t}_3, \boldsymbol{e}_{2,3}\} & 0 & 0 & \{\boldsymbol{z}_3, \boldsymbol{e}_{2,3}\} \end{bmatrix}$$

Compliance analysis

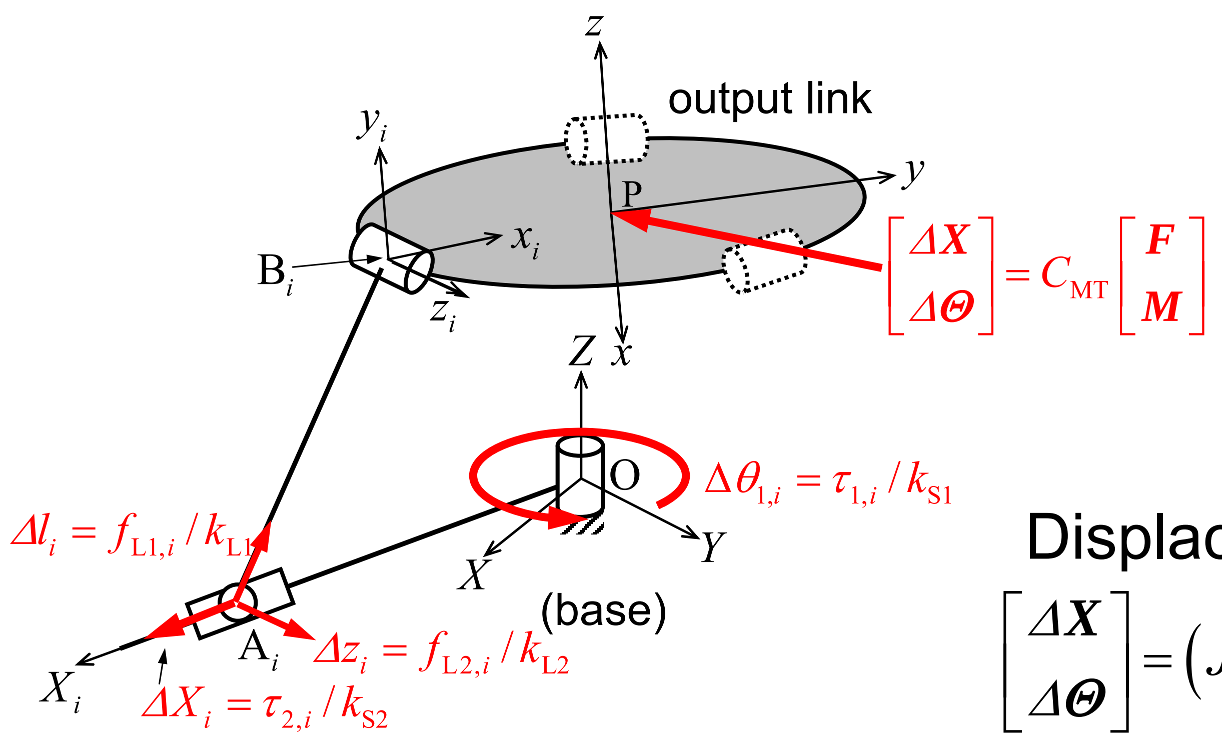

Forces and deformations

Displacement relationship:

$$\begin{bmatrix} \Delta X \\ \Delta \Theta \end{bmatrix} = \left(J_1^{\mathrm{T}}\right)^{-1} \begin{bmatrix} \Delta x_{L1} \\ \Delta x_{L2} \end{bmatrix} + \left(J^{\mathrm{T}}\right)^{-1} \begin{bmatrix} \Delta x_{S1} \\ \Delta x_{S2} \end{bmatrix}$$

Compliance model:

$$\begin{bmatrix} \Delta x_{L1} \\ \Delta x_{L2} \end{bmatrix} = -C_L \begin{bmatrix} f_{L1} \\ f_{L2} \end{bmatrix}, \quad C_L = \begin{bmatrix} \mathrm{diag.}[1/k_{L1}]_{3\times3} & 0_{3\times3} \\ 0_{3\times3} & \mathrm{diag.}[1/k_{L2}]_{3\times3} \end{bmatrix} \quad \text{(link compliance)}$$

$$\begin{bmatrix} \Delta x_{S1} \\ \Delta x_{S2} \end{bmatrix} = -C_S \begin{bmatrix} \tau_{S1} \\ \tau_{S2} \end{bmatrix}, \quad C_S = \begin{bmatrix} \mathrm{diag.}[1/k_{S1}]_{3\times3} & 0_{3\times3} \\ 0_{3\times3} & \mathrm{diag.}[1/k_{S2}]_{3\times3} \end{bmatrix} \quad \text{(servo compliance)}$$

Compliance analysis

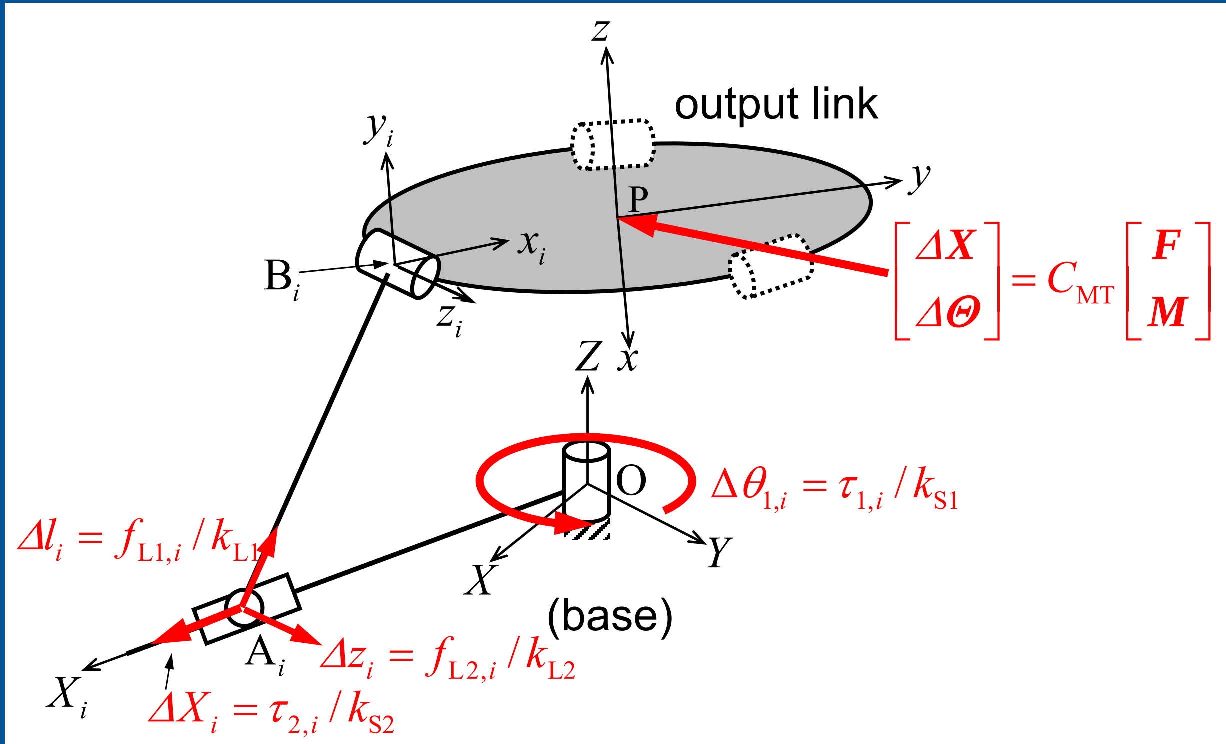

Forces and deformations

Compliance equation of the mechanism based on the VJM:

$$\begin{bmatrix} \Delta\boldsymbol{X} \\ \Delta\boldsymbol{\Theta} \end{bmatrix} = \left(J_1^{\mathrm{T}}\right)^{-1} \begin{bmatrix} \Delta\boldsymbol{x}_{\mathrm{L1}} \\ \Delta\boldsymbol{x}_{\mathrm{L2}} \end{bmatrix} + \left(J^{\mathrm{T}}\right)^{-1} \begin{bmatrix} \Delta\boldsymbol{x}_{\mathrm{S1}} \\ \Delta\boldsymbol{x}_{\mathrm{S2}} \end{bmatrix} = \left\{\left(J_1^{\mathrm{T}}\right)^{-1} C_{\mathrm{L}} J_1^{-1} + \left(J^{\mathrm{T}}\right)^{-1} C_{\mathrm{S}} J^{-1}\right\} \begin{bmatrix} \boldsymbol{F} \\ \boldsymbol{M} \end{bmatrix}$$

$$= \left(C_{\mathrm{ML}} + C_{\mathrm{MS}}\right) \begin{bmatrix} \boldsymbol{F} \\ \boldsymbol{M} \end{bmatrix} = C_{\mathrm{MT}} \begin{bmatrix} \boldsymbol{F} \\ \boldsymbol{M} \end{bmatrix}$$

Evaluation of compliance and pipe-bending accuracy

Tokyo Institute of Technology
Mechanical Systems Design Lab.

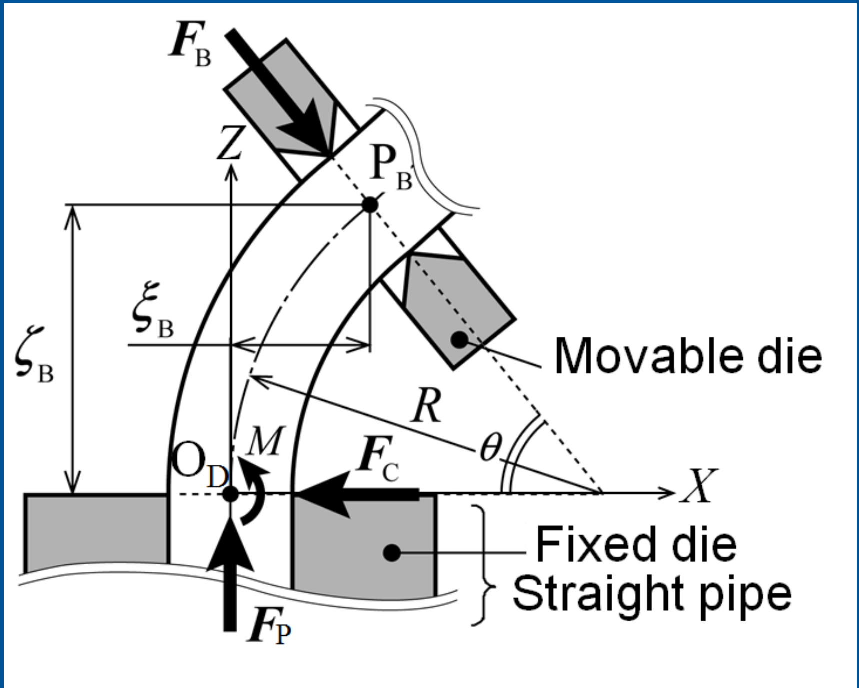

In-plane bending

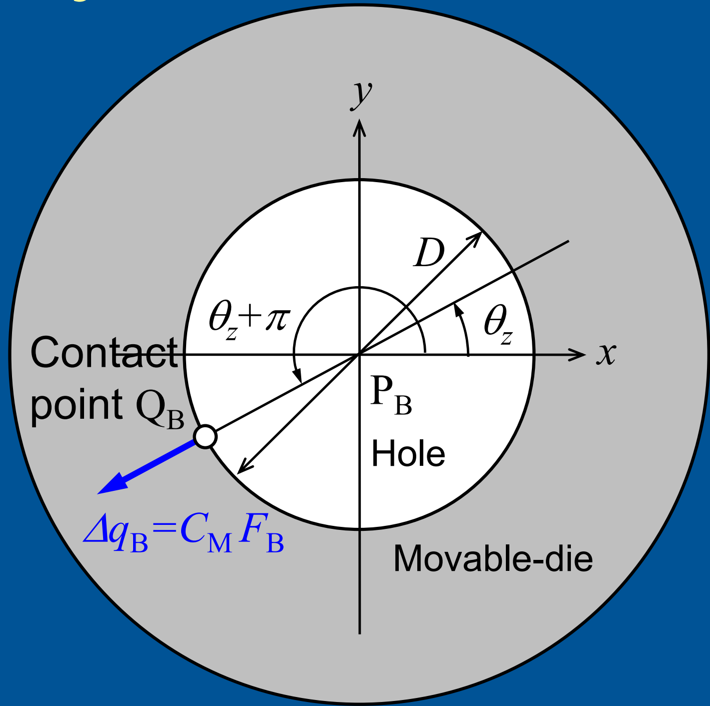

Force and displacement of Q_B

Displacement of Q_B in the direction of bending force:

$$\Delta q_B = \Delta \boldsymbol{q}_B^P \cdot \boldsymbol{e}_B^P = \left(R_P^T \Delta \boldsymbol{Q}_B\right) \cdot \boldsymbol{e}_B^P = \left\{R_P^T \left(\Delta \boldsymbol{P}_B + \Delta \boldsymbol{\Theta}_B \times \left(R_P \boldsymbol{q}_B^P\right)\right)\right\} \cdot \boldsymbol{e}_B^P$$

Displacement of P_B and angular displacement of output link by bending force:

$$\begin{bmatrix} \Delta \boldsymbol{P}_B \\ \Delta \boldsymbol{\Theta}_B \end{bmatrix} = C_{MT} \begin{bmatrix} \boldsymbol{F}_{B,P} \\ \boldsymbol{M}_{B,P} \end{bmatrix}$$

Evaluation of compliance and pipe-bending accuracy

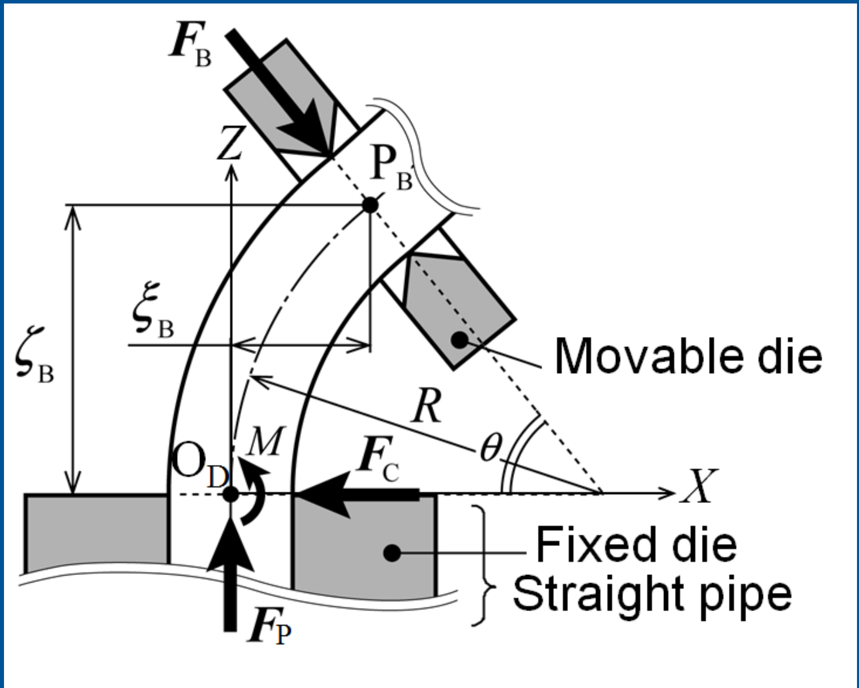

In-plane bending

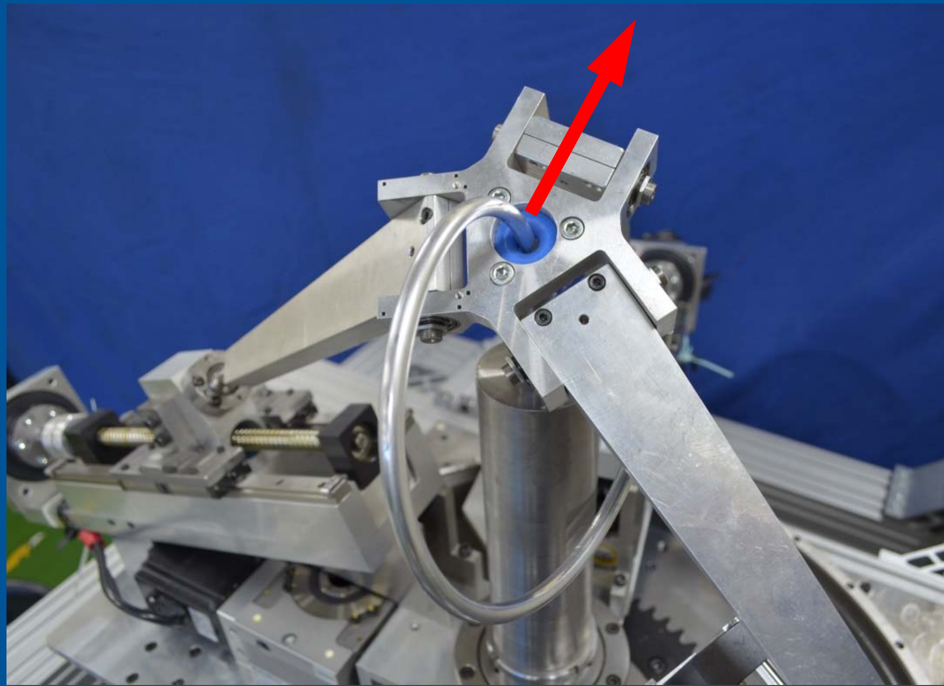

Direction of force

Displacement of Q_B in the direction of bending force:

$$\Delta q_B = \Delta \boldsymbol{q}_B^P \cdot \boldsymbol{e}_B^P = \left(R_P^T \Delta \boldsymbol{Q}_B \right) \cdot \boldsymbol{e}_B^P = \left\{ R_P^T \left(\Delta \boldsymbol{P}_B + \Delta \boldsymbol{\Theta}_B \times \left(R_P \boldsymbol{q}_B^P \right) \right) \right\} \cdot \boldsymbol{e}_B^P$$

Displacement of P_B and angular displacement of output link by bending force:

$$\begin{bmatrix} \Delta \boldsymbol{P}_B \\ \Delta \boldsymbol{\Theta}_B \end{bmatrix} = C_{MT} \begin{bmatrix} \boldsymbol{F}_{B,P} \\ \boldsymbol{M}_{B,P} \end{bmatrix}$$

Evaluation of compliance and pipe-bending accuracy

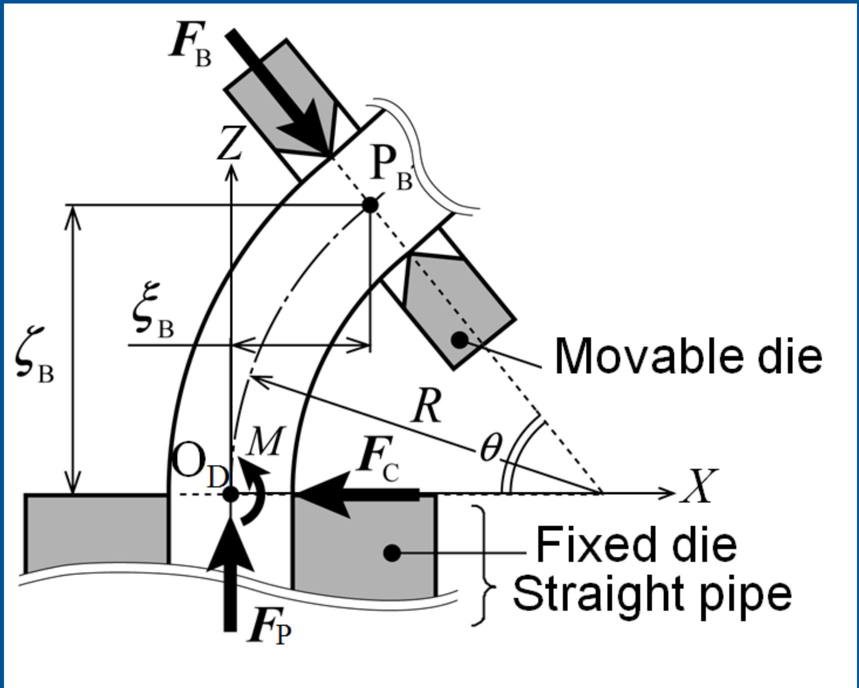

In-plane bending

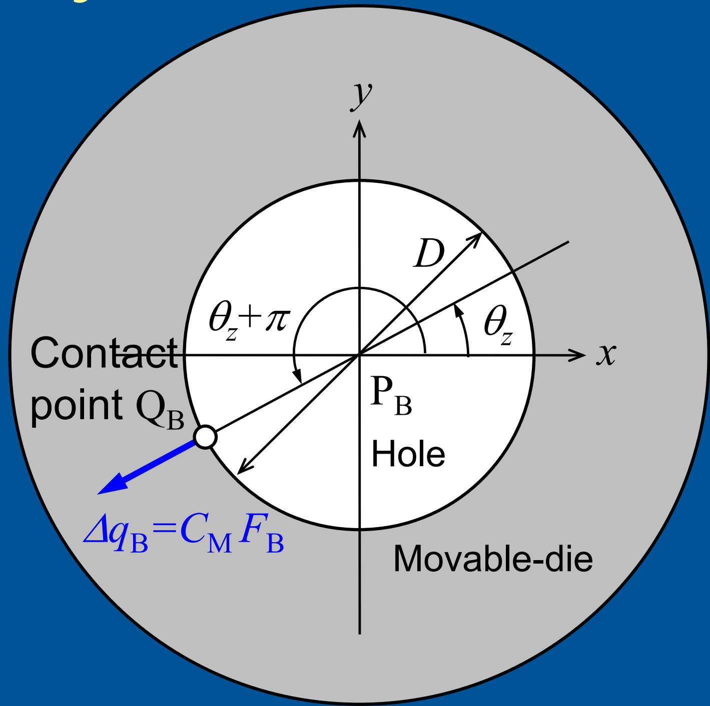

Force and displacement of Q_B

Compliance of the mechanism at the contact point Q_B:

$$C_M = \Delta q_B / F_B$$

Evaluation of compliance and pipe-bending accuracy

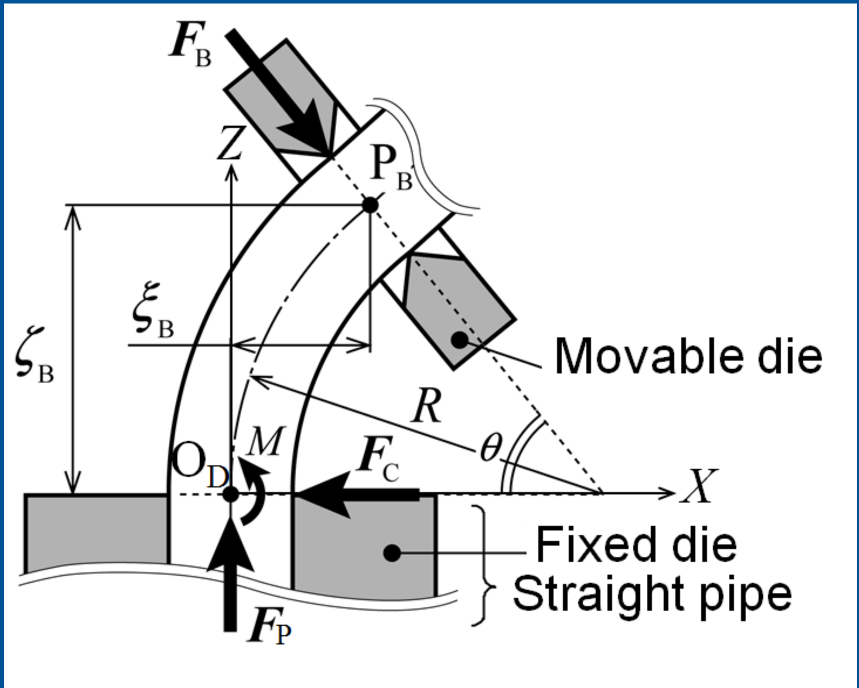

In-plane bending

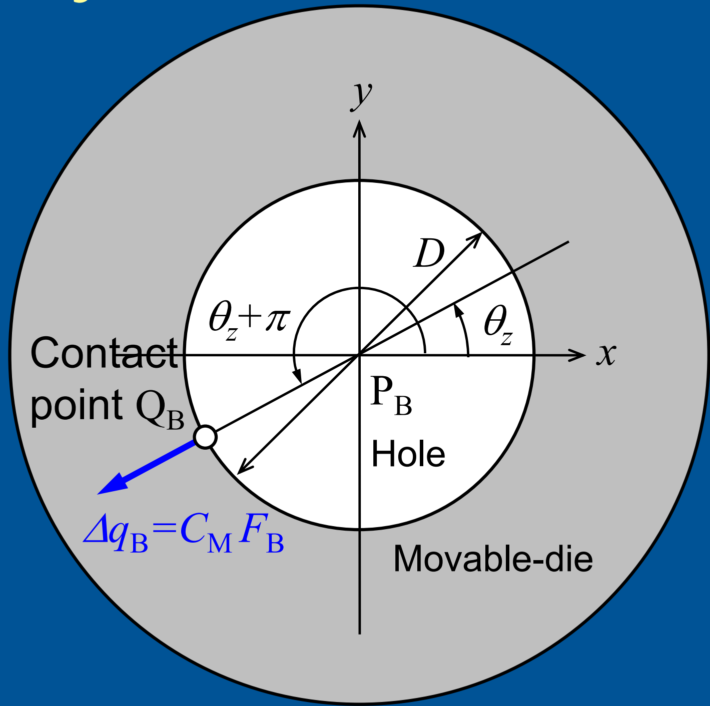

Force and displacement of Q_B

Index of curvature radius error caused by mechanism compliance:

$$\Delta R_M = \frac{\pi C_M}{2\theta \sin\theta}$$

Assumption: magnitude of the moment *M* required for bending a pipe into the same curvature radius *R* is the same even if the angle θ is different.

Results of compliance evaluation

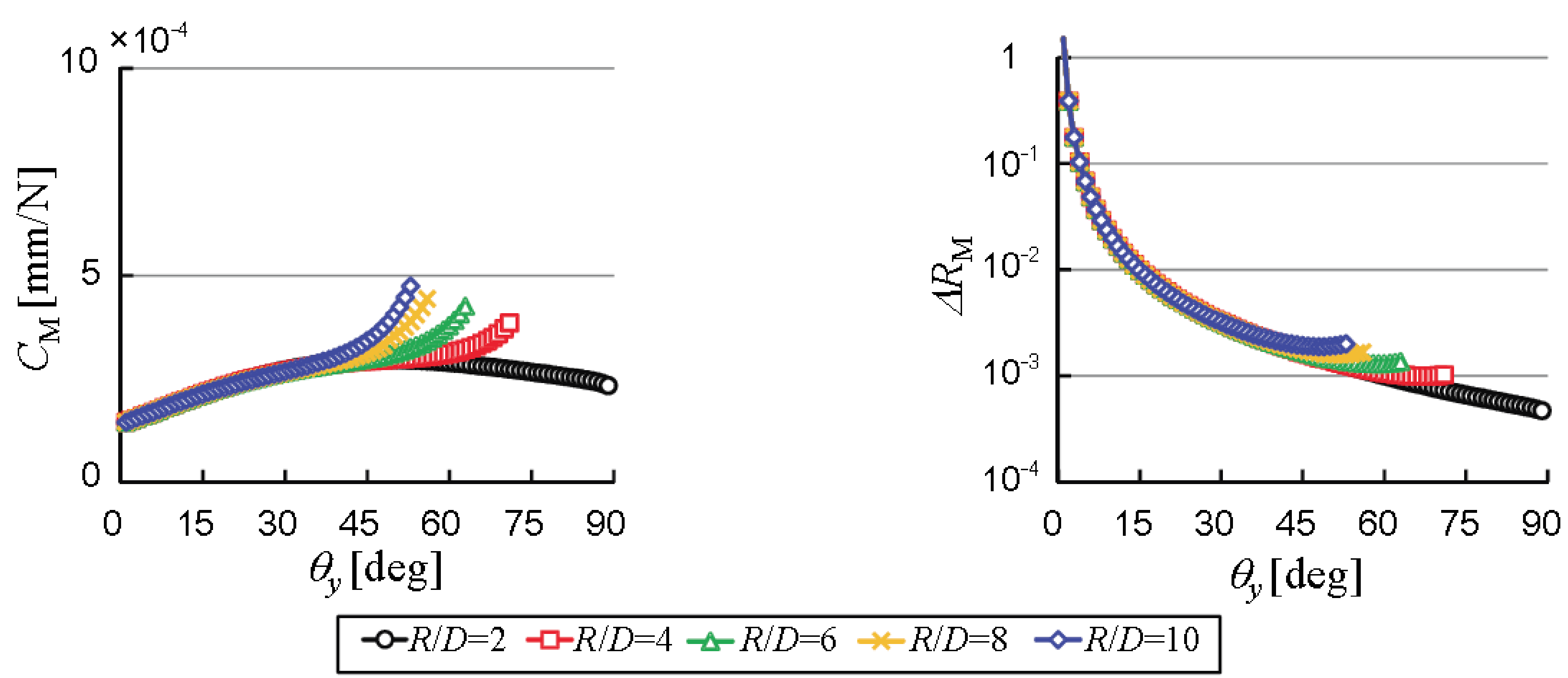

Compliance and curvature accuracy vs. inclination angle and radius of curvature of bent pipe

Parameter values used in the calculation

parameter	value	parameter	Value
r	45 mm	k_{L1}	1.6×10^5 N/mm
l	260 mm	k_{L2}	5.4×10^2 N/mm
β_B	20 deg	k_{S1}	3.6×10^7 N mm/rad
z_{PB}	0 mm	k_{S2}	1.0×10^4 N/mm

Results of compliance evaluation

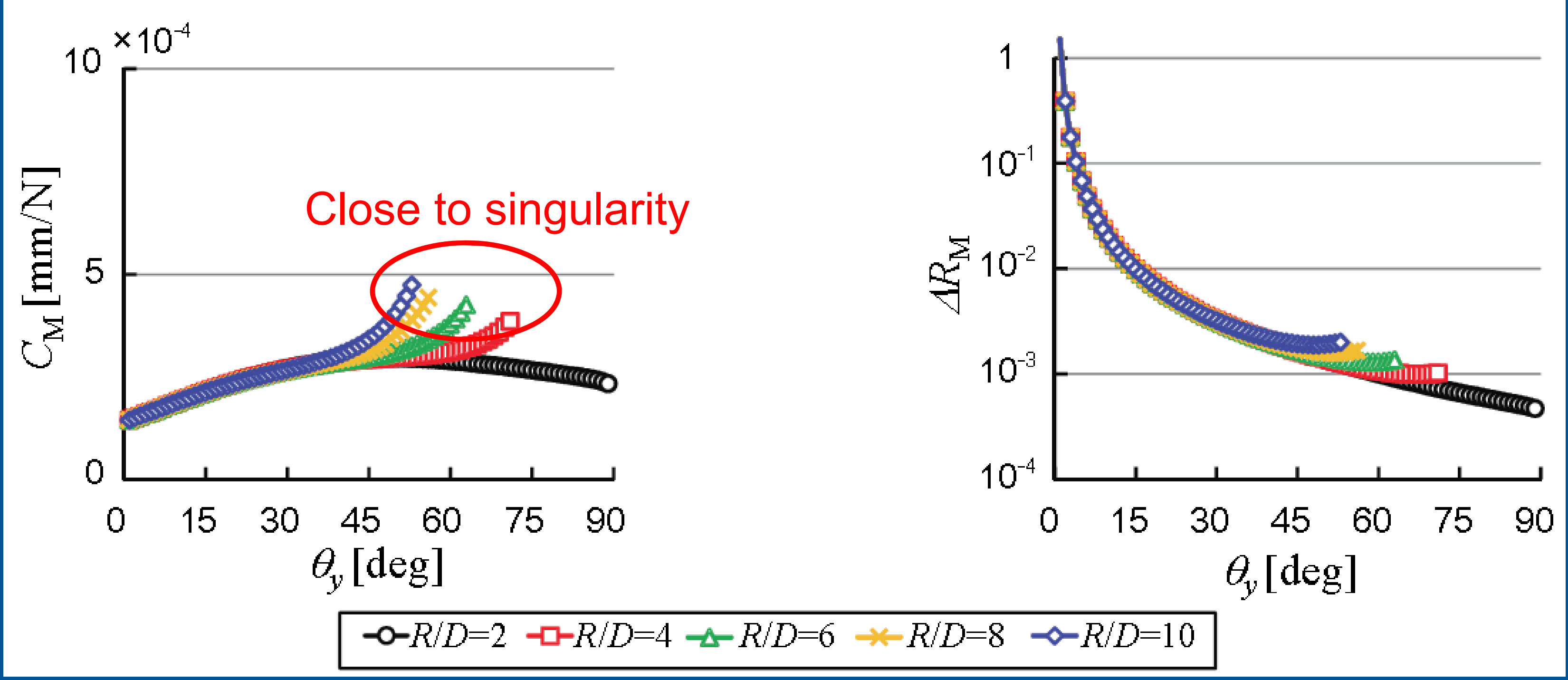

Compliance and curvature accuracy vs. inclination angle and radius of curvature of bent pipe

[Compliance]

(1) Compliance characteristics are stable in a wide range of θ_y except for the areas closed to singularity

(2) Compliance characteristics at $R/D=2$ are quite stable in the whole range of θ_y. This means that there is a wide selection in bending conditions for fabricating pipes with complex shapes.

Results of compliance evaluation

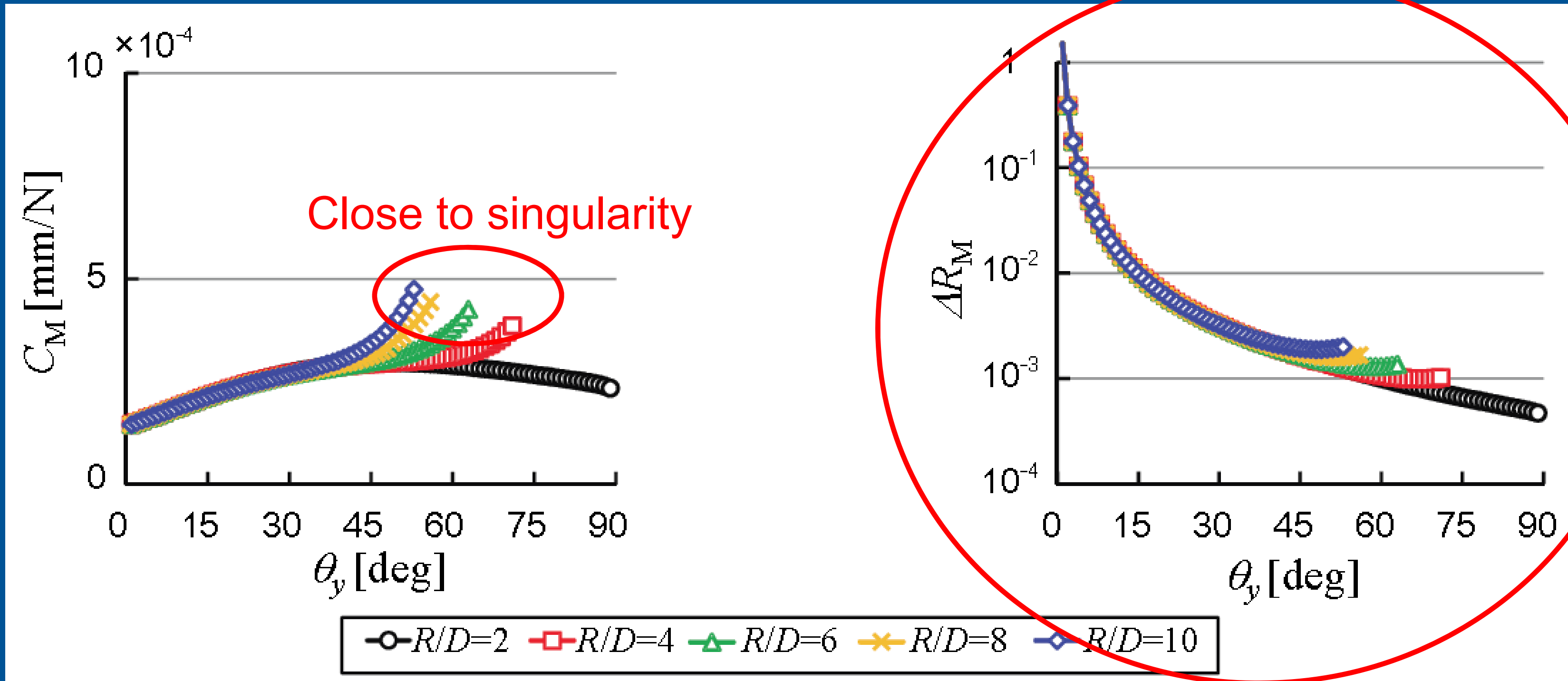

Compliance and curvature accuracy vs. inclination angle and radius of curvature of bent pipe

[Curvature radius error]

(1) ΔR_M monotonously reduces according to the increase of θ_y for all conditions of R/D.

(2) Our mechanism performs better in terms of the curvature radius error by selecting the angle θ_y as large as possible for all R/D.

Experiments

Tokyo Institute of Technology
Mechanical Systems Design Lab.

Purpose: to investigate the effect of the angle θ_y on the accuracy of the bent pipe.

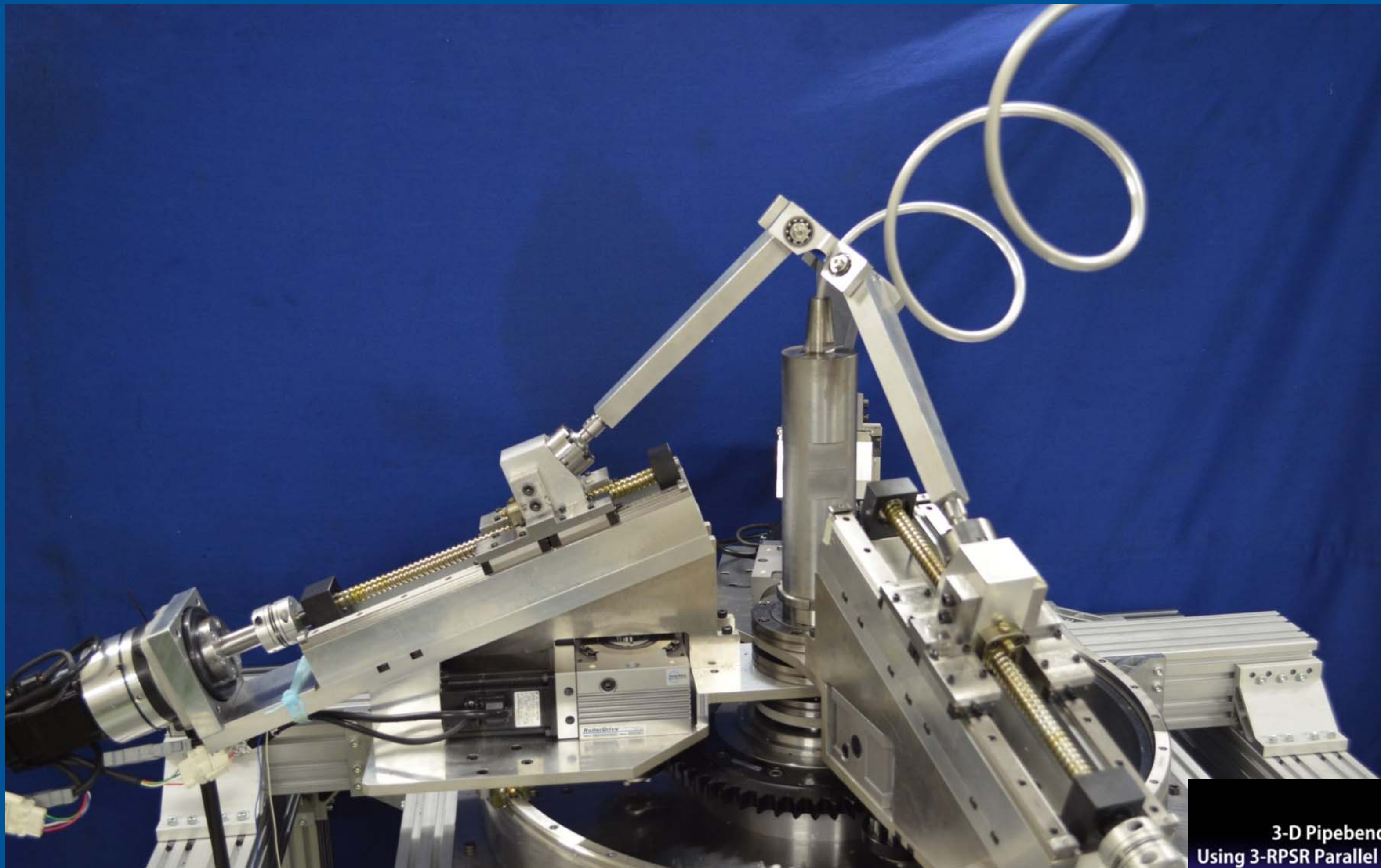

Bending by the 3rd prototype

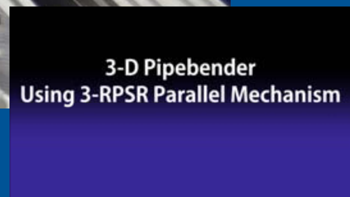

Experiments

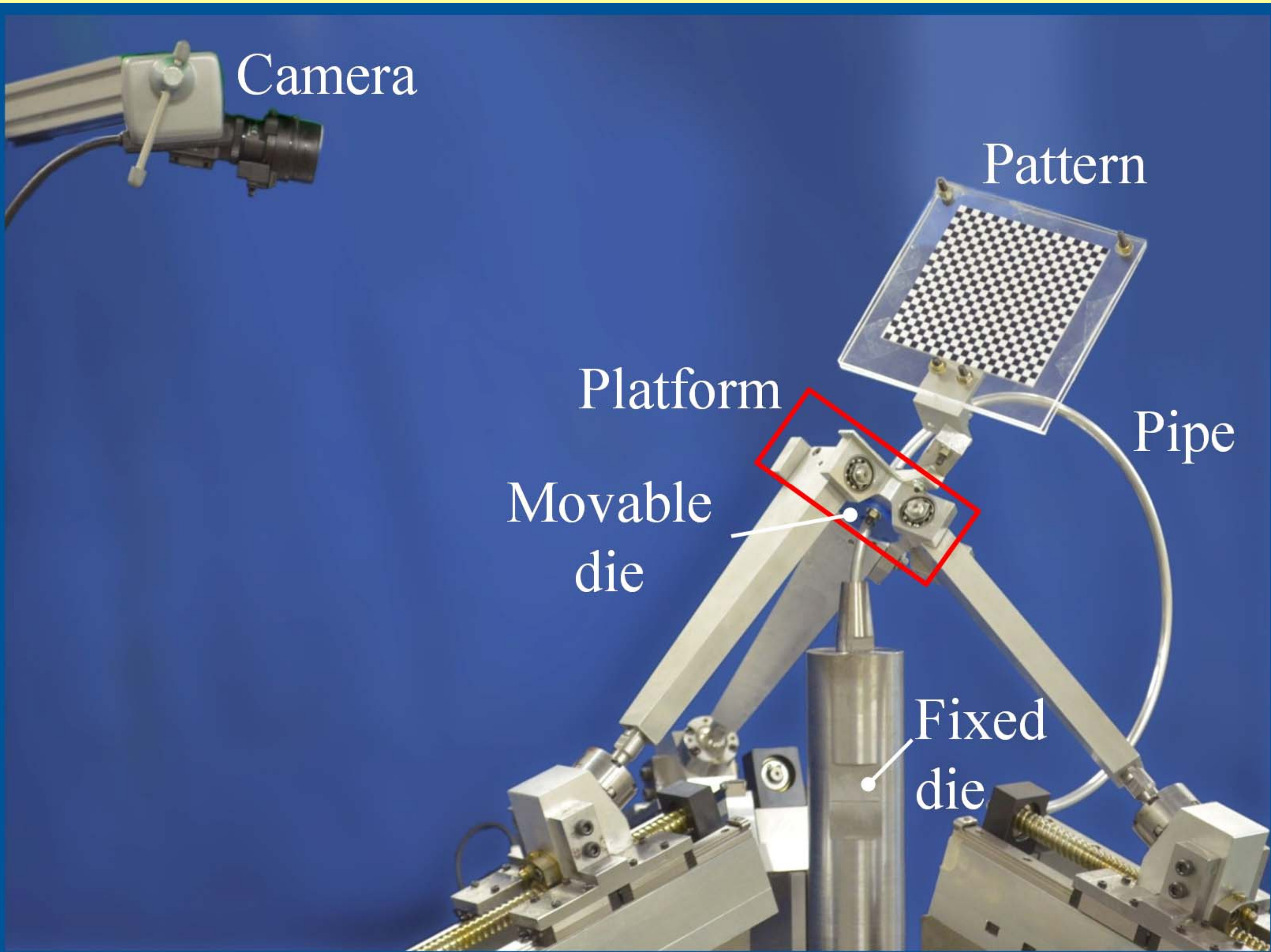

Pose measurement system during bending using checker pattern and camera (Details will be presented at the session FrB1 "Calibration")

Experiments

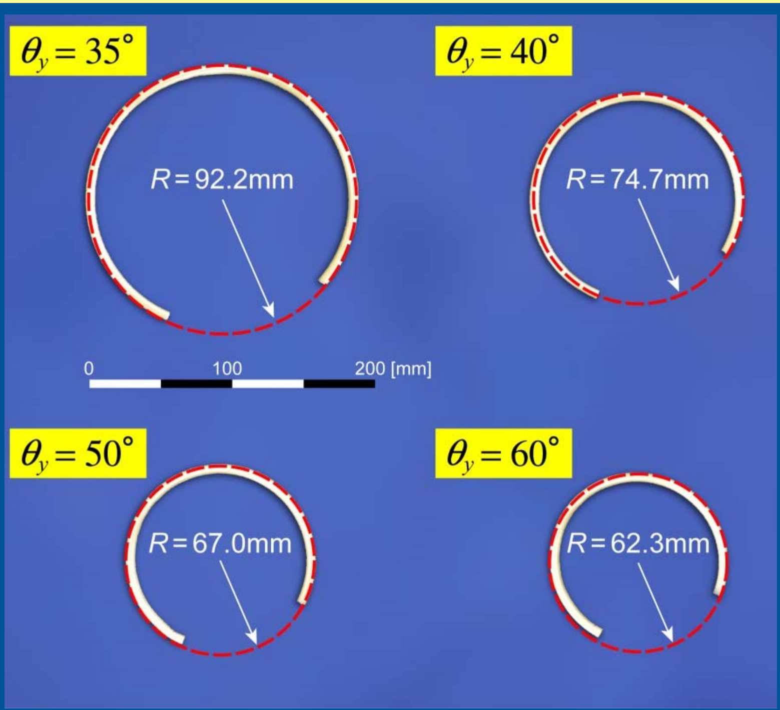

Bent pipes (R=50 mm)

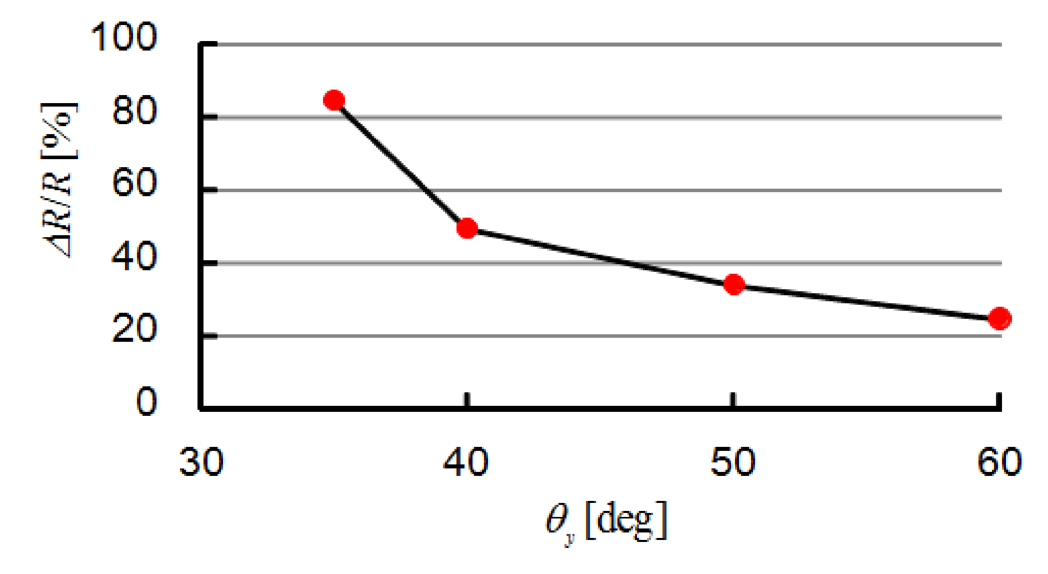

Curvature radius error of bent pipes

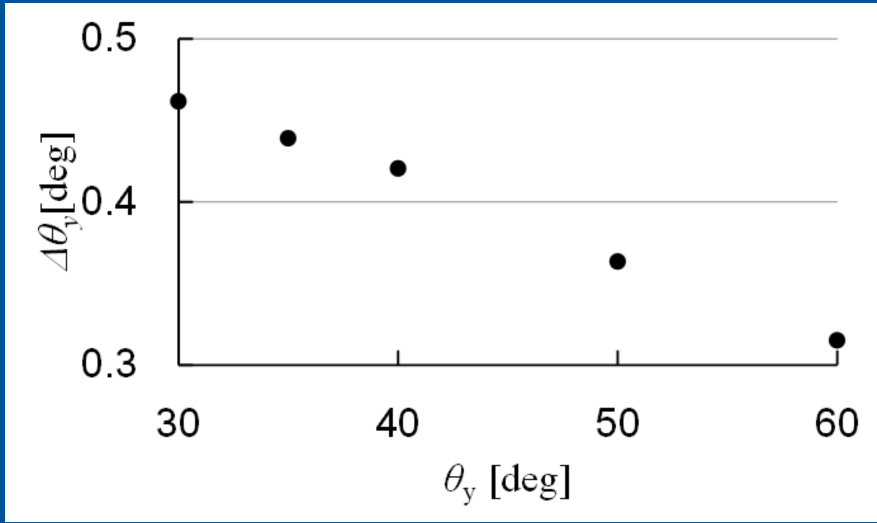

Orientation error during bending

It is known from the figures that the angle θ_y has great effects on the pose accuracy of the movable-die and the shape accuracy of the bent pipe. That is, accuracy of bending is improved by setting θ_y at an angle as large as possible. This result supports the theoretical results.

Summary-Compliance Analysis

Compliance characteristics of the 3-RPSR mechanism and fabrication error of bent pipes using this mechanism have been theoretically and experimentally investigated. Our conclusions are summarized as follows.

1. Evaluation indices for compliance characteristics and curvature radius error of the movable-die drive mechanism have been proposed. Based on the indices, effects of the bending conditions, such as the target radius of curvature of bent pipe and inclination angle of the movable die, on these performances of the mechanism have been clarified. As the result, it was clarified that the mechanism has a good characteristics as the movable-die drive mechanism of a pipe bender especially for fabricating pipes with small curvature radii.
2. Experimental results using the prototype pipe bender have shown to support the theoretical results.

Table of contents

Problems for Precise Bending

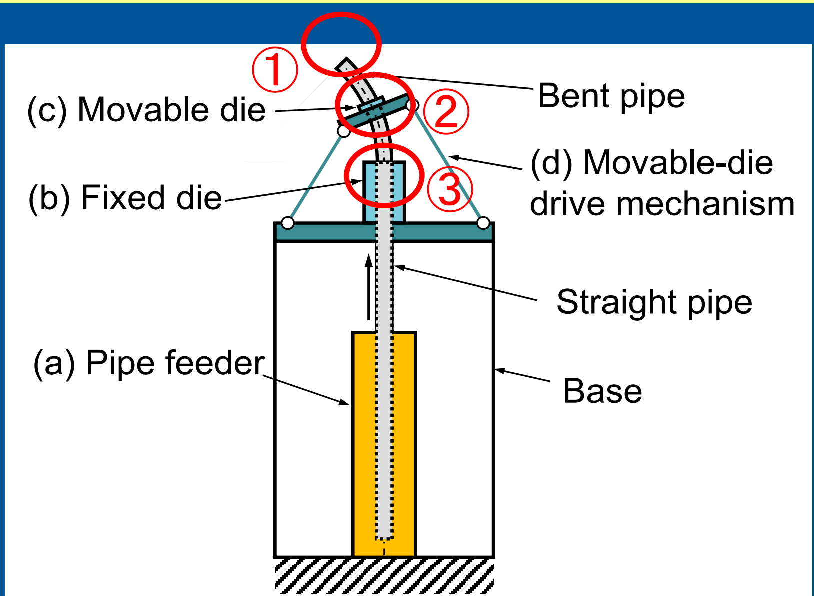

Pipe Bender

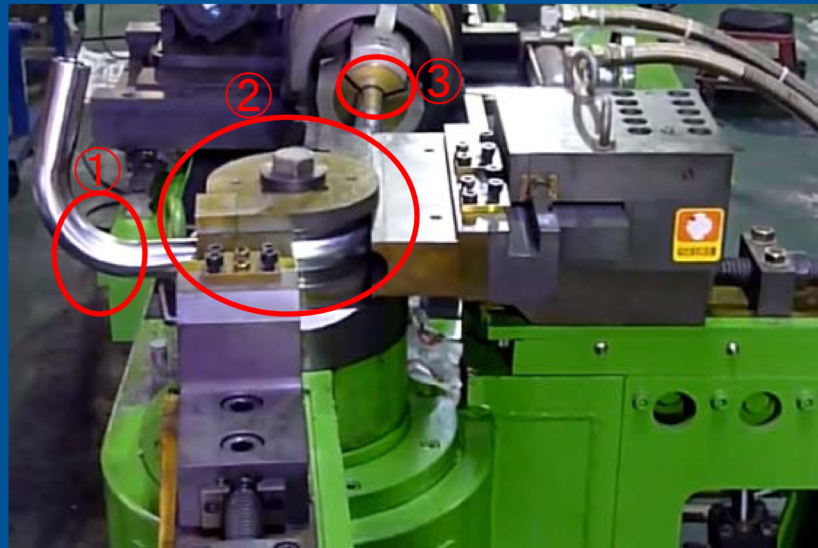

Draw bender（Taiyo Co., Ltd.）

Error sources and points of interests：

① Springback effect of pipe（previous work: compensation based on preliminary experiments）

② Clearance between pipe and movable die（Draw bending: large contact area, Penetration bending: point contact）

③ Clearance between pipe and fixed die

Purpose of the work

Tokyo Institute of Technology
Mechanical Systems Design Lab.

Determination of the compensated pose of the movable die, taking into consideration the error sources, for desired shape of bent pipe to achieve precise pipe-bending.

1. A model for estimating the bent pipe’s shape and bending force, taking into consideration the clearance at the dies as well as the springback of pipe, is proposed.
2. Based on the results, a strategy for determining the pose of the movable-die drive mechanism as the feed-forward information is proposed.
3. Experiments for fabricating pipes of several target shapes have been conducted, and results are discussed in terms of accuracy of the bent shape.

Target pipe:

- ✓ Aluminum(A6063)
- ✓ Uniform circular cross-section(outer diameter=8mm, thickness=1mm)
- ✓ Bent pipe in a plane(constant and variable radius of curvature)

Penetration Bending Model

Conditions:

1. Relationship between the stress and strain
2. Bending moment applied on the pipe
3. Springback formulation
4. Contact condition of pipe and the dies

To obtain:

- Input: pose of the movable die
  Including conditions:
  property of pipe (dia., Young's modulus, etc.), clearance
- Output: Shape of the bent pipe

Usage: To determine in a feed-forward way the pose of the movable die according to the target shape of the bent pipe.

Penetration Bending Model

Relationship between the stress and strain:

$$\sigma = \begin{cases} E\varepsilon \quad (\varepsilon \leq \varepsilon_y) & \text{: elastic area} \\ C\varepsilon^n \quad (\varepsilon_y < \varepsilon) & \text{: plastic area} \end{cases}$$

Penetration Bending Model

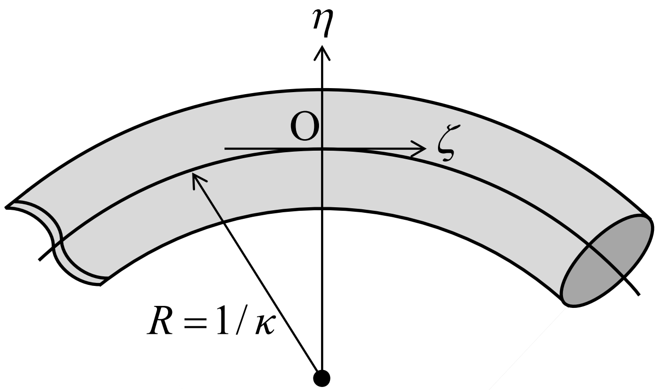

Bent pipe with a constant curvature

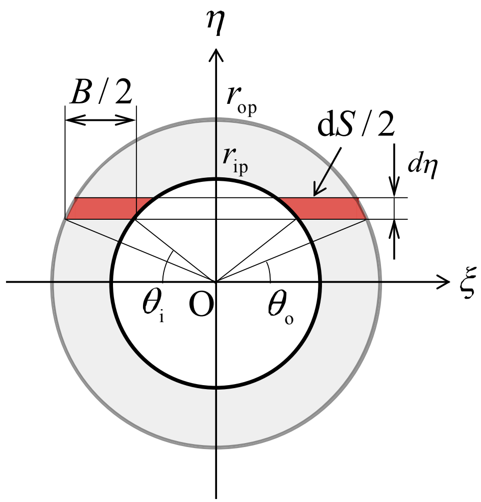

Cross section of bent pipe

Bending moment M to bend a pipe of curvature κ:

$$M = f_\kappa(\kappa) = \int_S \sigma(\varepsilon)\eta\, dS = 2\int_0^{r_{op}} \sigma(\kappa\eta)\eta\, B(\eta) d\eta$$

$$\varepsilon = \kappa\eta$$

$$B = \begin{cases} 2(r_{op}\cos\theta_o - r_{ip}\cos\theta_i) & (\ 0 \le \eta \le r_{ip}) \\ 2\quad r_{op}\cos\theta_o & (r_{ip} \le \eta \le r_{op}) \end{cases}, \text{ where } \theta_o = \sin^{-1}\left(\frac{\eta}{r_{op}}\right), \quad \theta_i = \sin^{-1}\left(\frac{\eta}{r_{ip}}\right)$$

Penetration Bending Model

Tokyo Institute of Technology
Mechanical Systems Design Lab.

Springback and Clearance at fixed die is considered.

Curvature: $\kappa(s) = \kappa_{\max} - \kappa^*(s)$

Springback: $\kappa^*(s) = \dfrac{M(0) - M(s)}{EI}$

$$M_{\max} = f_\kappa(\kappa_{\max}) = \boldsymbol{r}(0) \times \boldsymbol{F}_{\mathrm{md}}$$

$$M(s) = \begin{cases} \boldsymbol{r}(s) \times \boldsymbol{F}_{\mathrm{md}} & (0 \le s \le s_{\mathrm{n}}) \\ 0 & (s_{\mathrm{n}} < s \quad) \end{cases}$$

where $\boldsymbol{r}(s) = \boldsymbol{Q}(s_{\mathrm{n}}) - \boldsymbol{Q}(s)$

Center line:

$$\boldsymbol{Q}(s) = \begin{bmatrix} x_{\mathrm{Q}} \\ y_{\mathrm{Q}} \end{bmatrix} = \begin{bmatrix} 0 \\ \Delta r_{\mathrm{if}} \end{bmatrix} + \int_0^s \begin{bmatrix} \cos\phi(l) \\ \sin\phi(l) \end{bmatrix} dl$$

$$\phi(s) = \phi_0 + \int_0^s \kappa(l)\,dl$$

ϕ_0: deformation angle at $s = 0$

Δr_{if}: clearance at fixed die

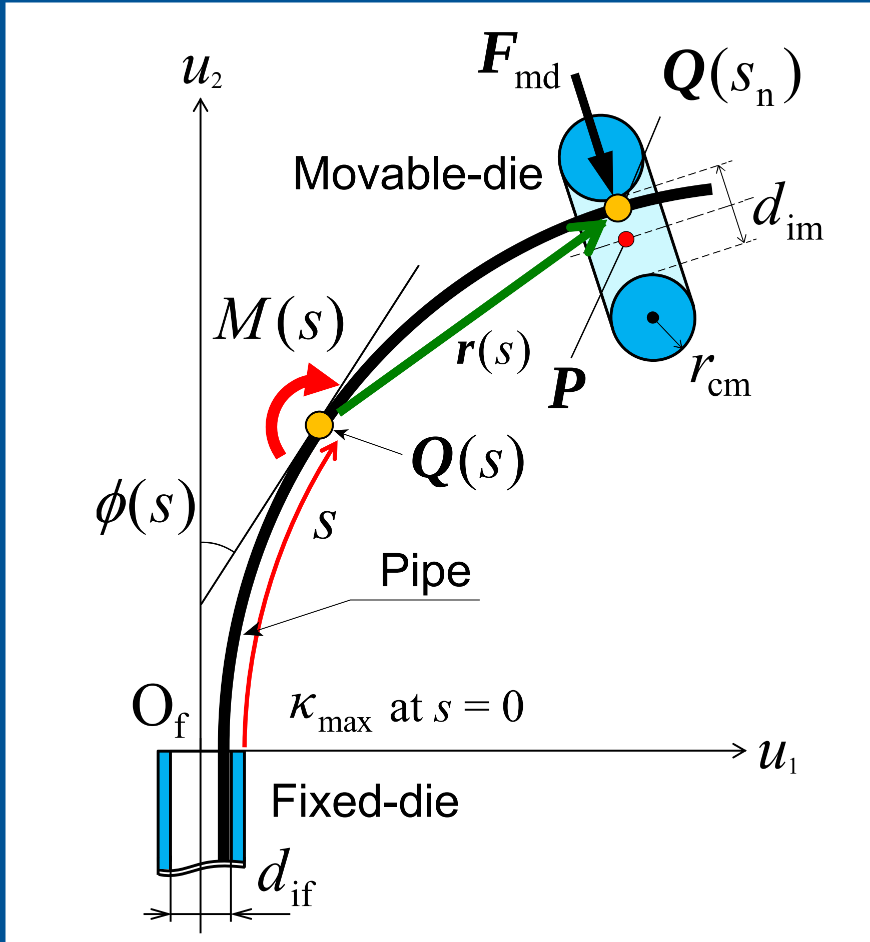

Penetration bending model

The centerline of pipe (bold line) can be determined by assumed values $\kappa_{\max}$ (curvature at the exit of the fixed die) and s_{n} (arc length of the contact point of pipe with movable die).

Flowchart-1

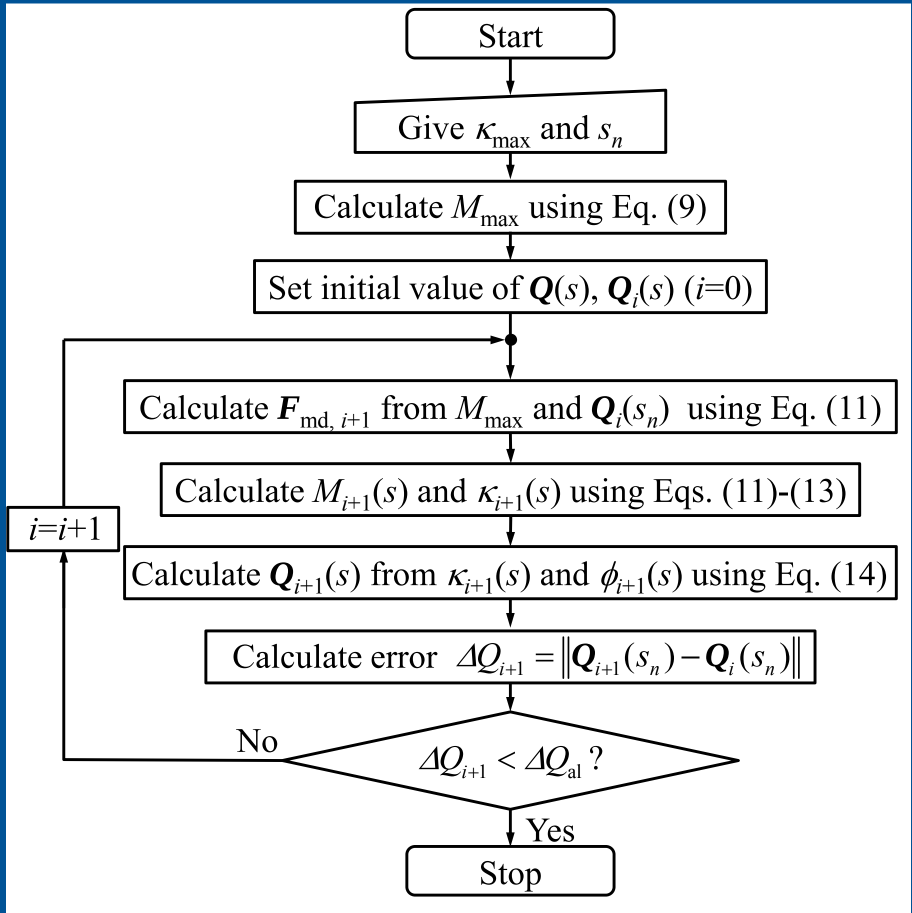

Flowchart to calculate centerline of bent pipe $\boldsymbol{Q}(s)$ from given set of the maximum curvature κ_{max} and position of the contact point s_n.

Once the two values κ_{max} and s_n are assumed, maximum bending moment M_{max}, bending force $\boldsymbol{F}_{md}$, bending moment distribution $M(s)$ and curvature distribution $\kappa(s)$ are calculated step by step using equations shown in the figure where i and ΔQ_{al} denote increment number of iteration and allowable error of convergence. Let us note that κ_{max} and s_n cannot be freely specified, but should be determined based on the contact condition between pipe and dies. Determination of these values is discussed in the following.

Calculation of Center Line of Bent Pipe

Tokyo Institute of Technology
Mechanical Systems Design Lab.

Pose of and clearance at movable die is considered.

Center line is obtained such that the outer surface of the pipe is tangential to the contact surface of the movable die.

Input: pose of movable die(u_1, u_2, θ_y)

Output: centerline $\boldsymbol{Q}(s)$, force F_{md}

Resultant curvature: $\kappa_{\mathrm{d}} = \kappa_{\min} = \kappa\,(s_{\mathrm{n}})$

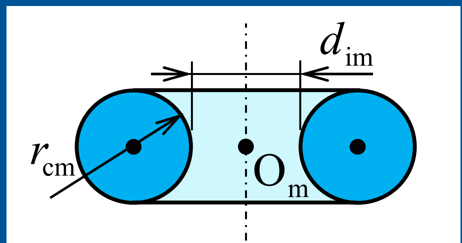

Cross section of movable die

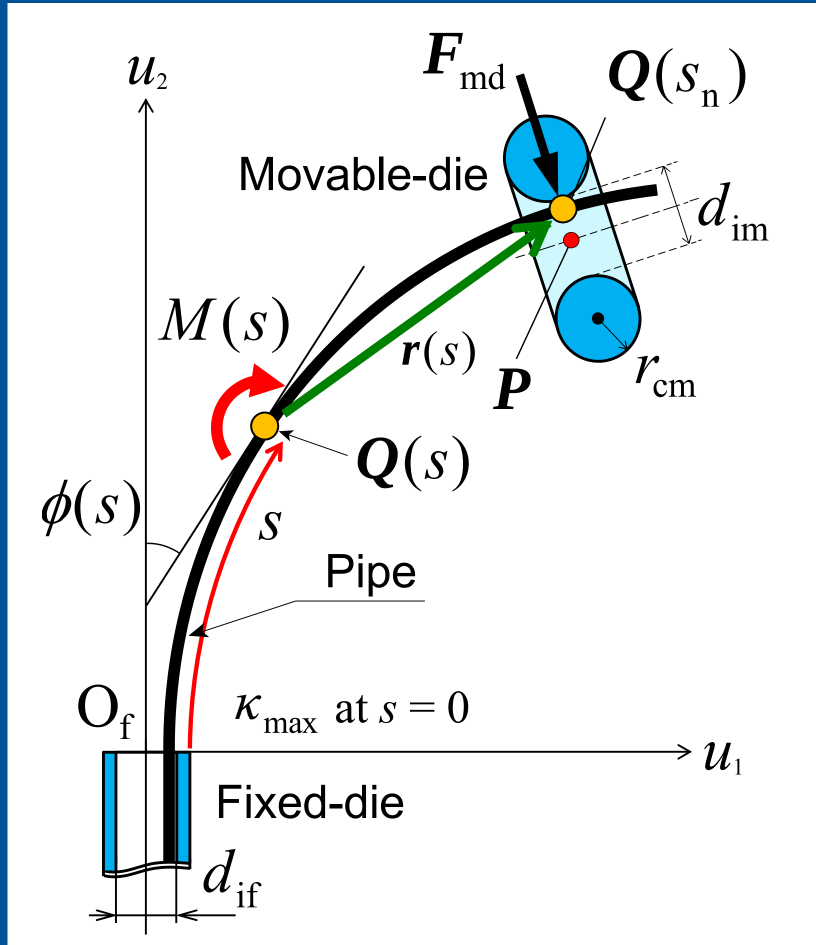

Penetration bending model

The centerline of pipe (bold line) can be determined by assumed values $\kappa_{\max}$ (curvature at the exit of the fixed die) and s_{n} (position of the contact point of pipe with movable die). Procedure to determine $\kappa_{\max}$ and s_{n} is presented next.

Flowchart-2

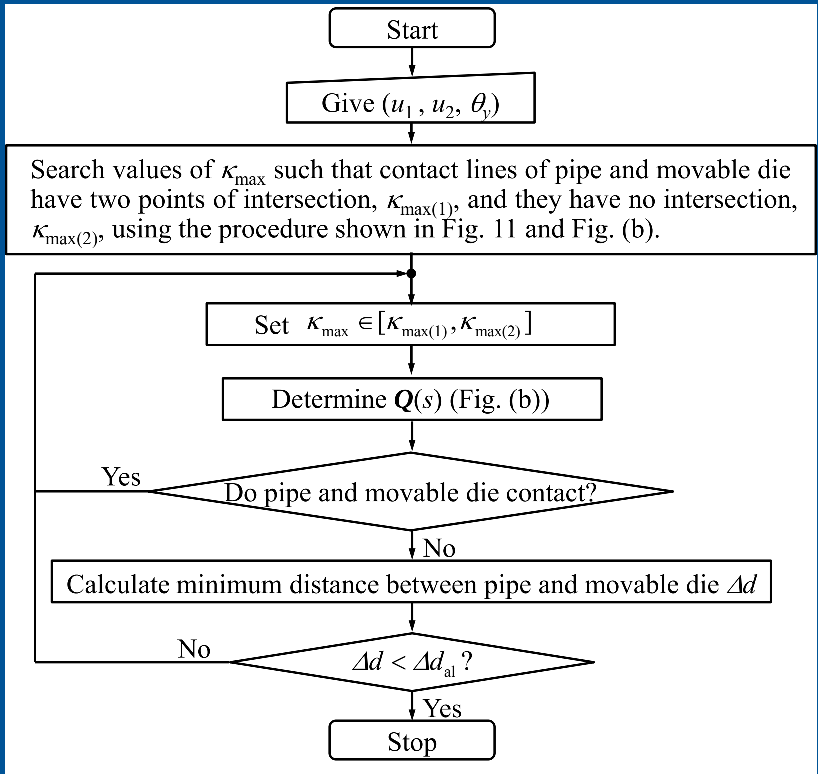

(a) flowchart to determine pipe's shape

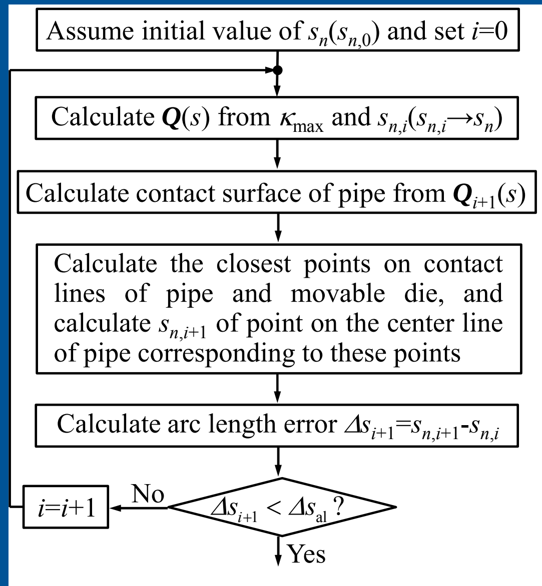

(b) flowchart to determine centerline of pipe

Flowchart to determine bent pipe's shape from given pose of movable die taking into consideration springback of pipe and clearances between pipe and dies.

Figure (a) shows the total procedure. Centerline of pipe is obtained in Figure (b) so that distance between the assumed contact point on the pipe and the contact line of movable die is minimized for given pose of movable die (u_1, u_2, θ_y) and maximum curvature κ_{max}.

Numerical Example

Material and dies parameters

Material of pipe : A6063			
Young's modulus E [GPa]	70	Outer diameter d_{op}[mm]	8.0
Yield strain ε_y [%]	0.25	Inner diameter d_{ip}[mm]	6.0
Work-hardening exponent n	0.15		
Fixed die (SKD)		Movable die (MC Nylon)	
Inner diameter d_{if} [mm]	8.3	Inner diameter d_{im}[mm]	8.3
Deflection angle at the exit of fixed- die ϕ_0 [deg]	※ 1.8		

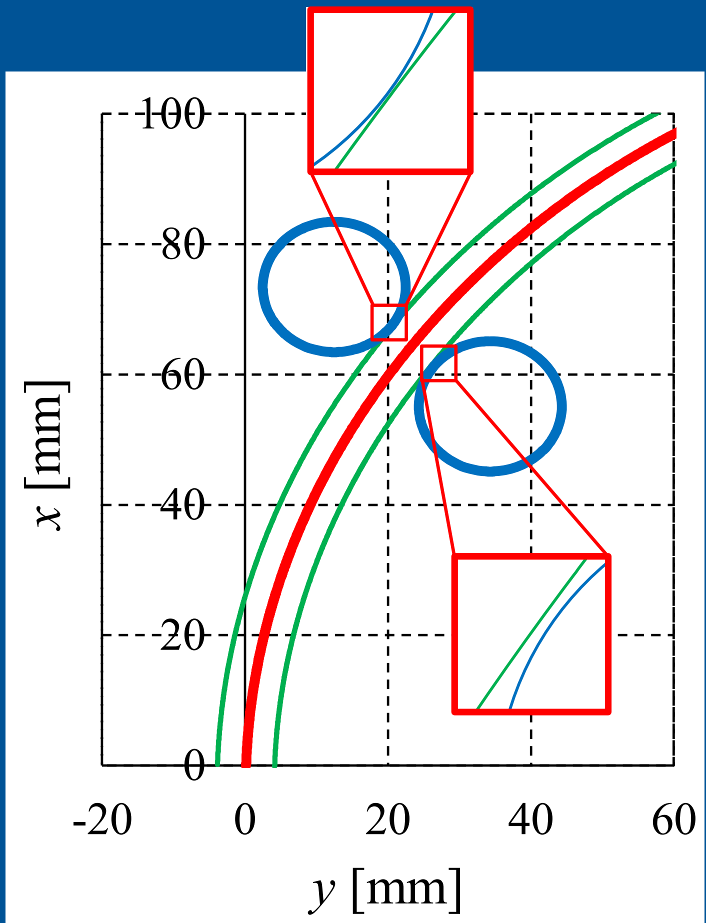

Result (R_g=100 mm, θ_y=40 deg)

In the figure, the solid red and thin green lines represent center and outer lines of the pipe, and two blue circles represent contact lines of movable die, respectively. From the enlarged views, it is known that the pipe contacts the movable die only at one point.

Estimation of the Bent Pipe's Shape and Bending Force

Workspace of movable-die drive mechanism

Geometrical condition of mechanism and singularity

➡ $\theta_{y,\max}$

Collision of pipe with fixed and movable dies

➡ $\theta_{y,\min}$

Distribution of pipe's curvature and bending force in the workspace were estimated by the proposed method.

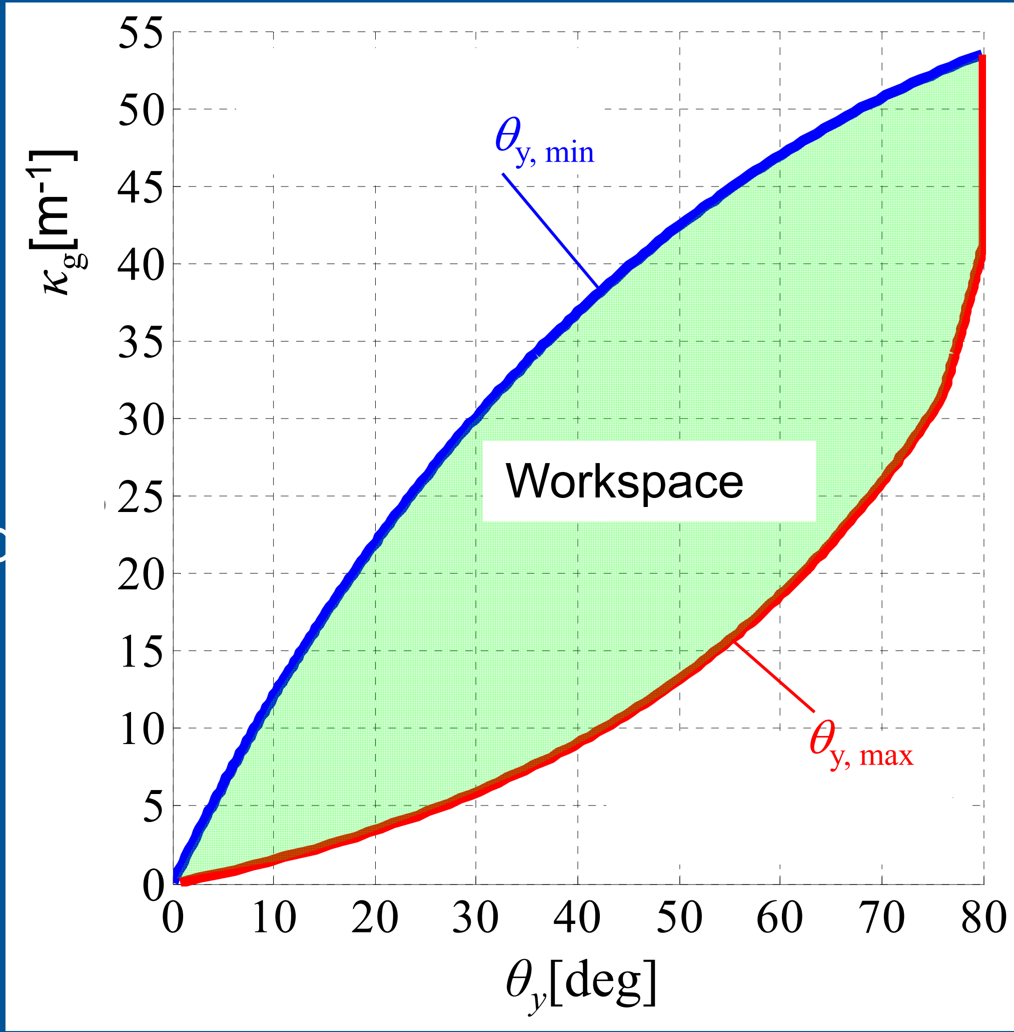

Workspace of movable-die drive mechanism

Estimation of the Bent Pipe's Shape and Bending Force

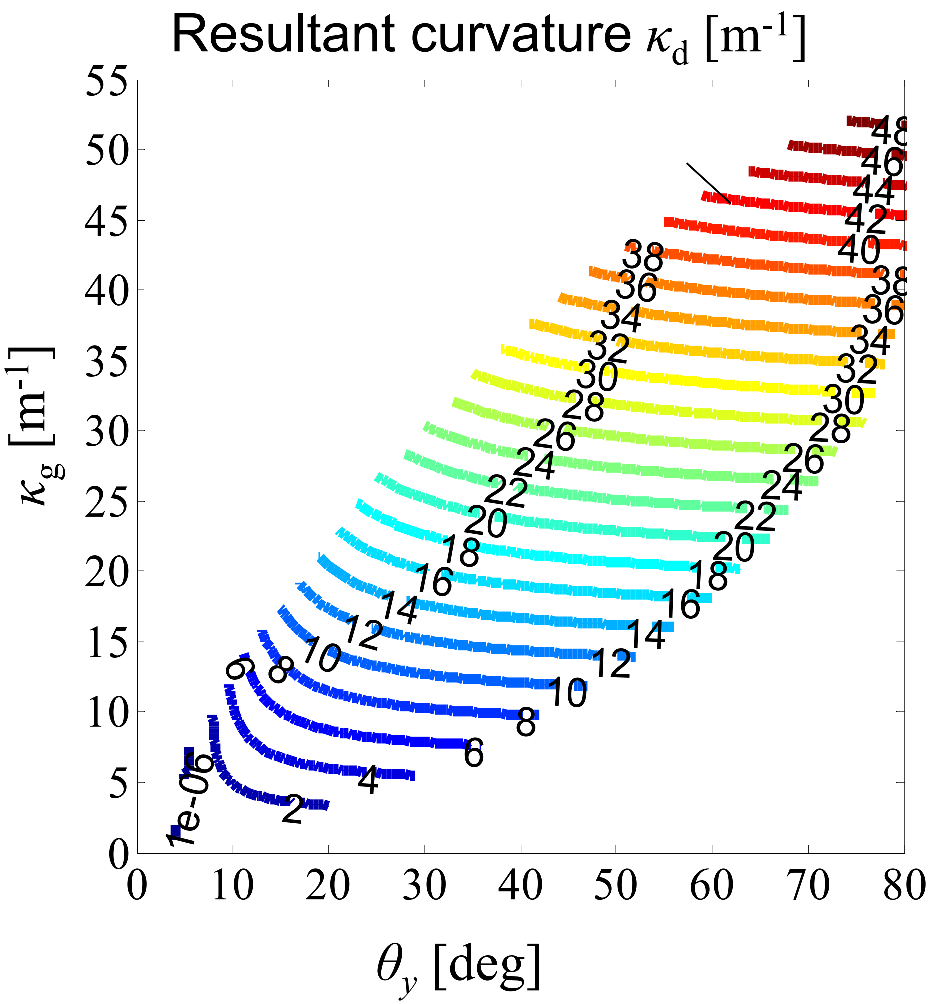

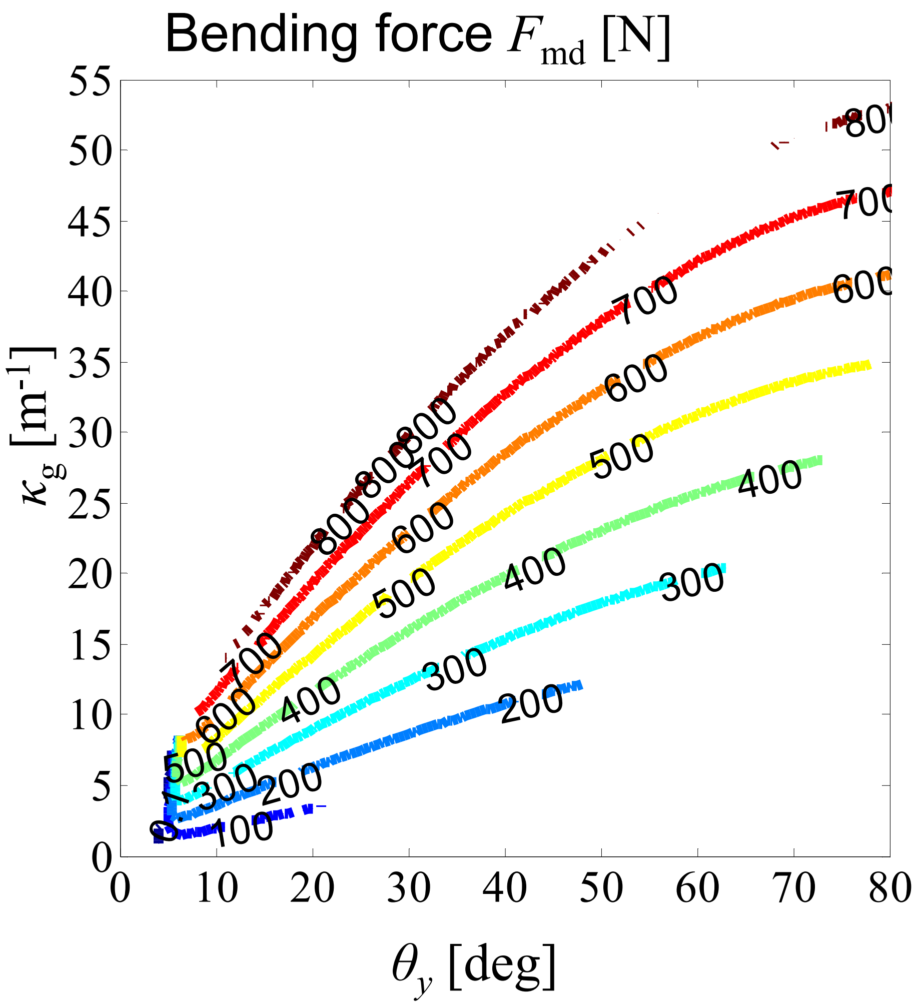

Results of calculation

Strategy for Determining Movable Die's Pose

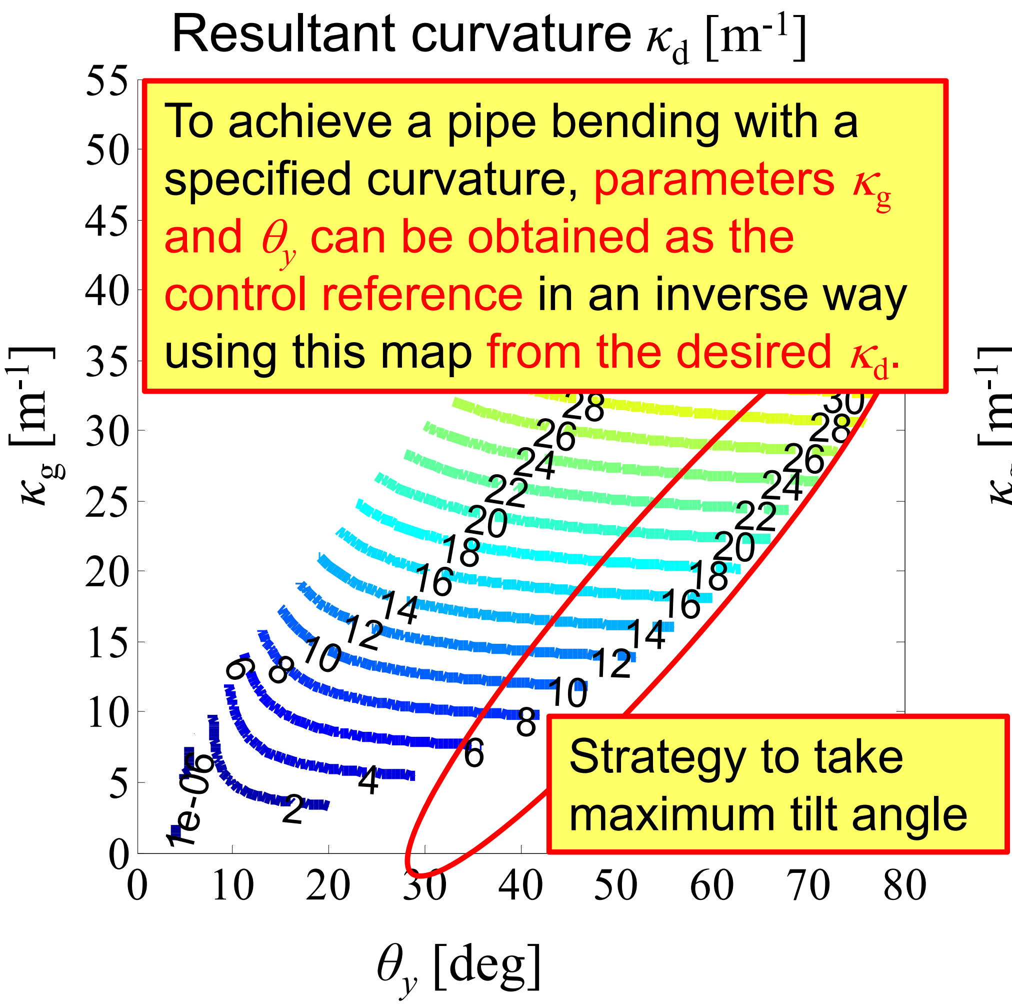

To achieve a pipe bending with a specified curvature, parameters κ_g and θ_y can be obtained as the control reference in an inverse way using this map from the desired κ_d.

Strategy to take maximum tilt angle

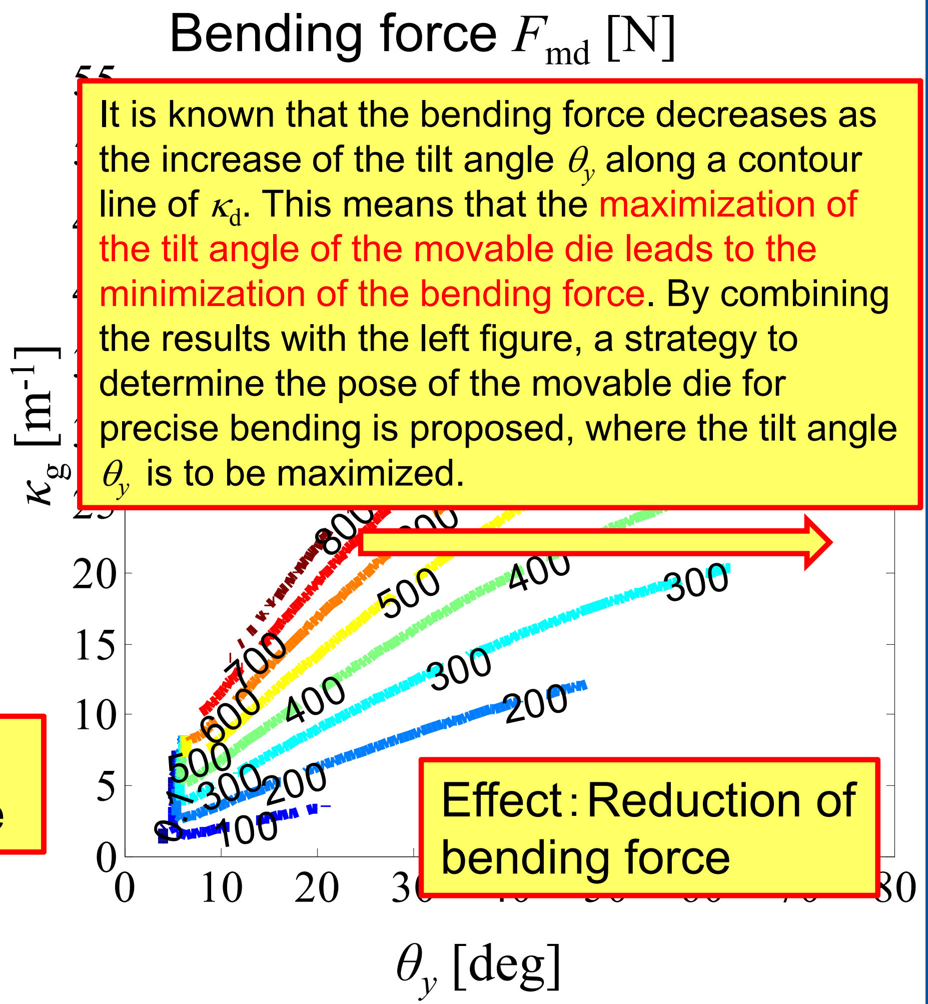

It is known that the bending force decreases as the increase of the tilt angle θ_y along a contour line of κ_d. This means that the maximization of the tilt angle of the movable die leads to the minimization of the bending force. By combining the results with the left figure, a strategy to determine the pose of the movable die for precise bending is proposed, where the tilt angle θ_y is to be maximized.

Effect : Reduction of bending force

Results of calculation

Strategy for Determining Movable Die's Pose

Tokyo Institute of Technology
Mechanical Systems Design Lab.

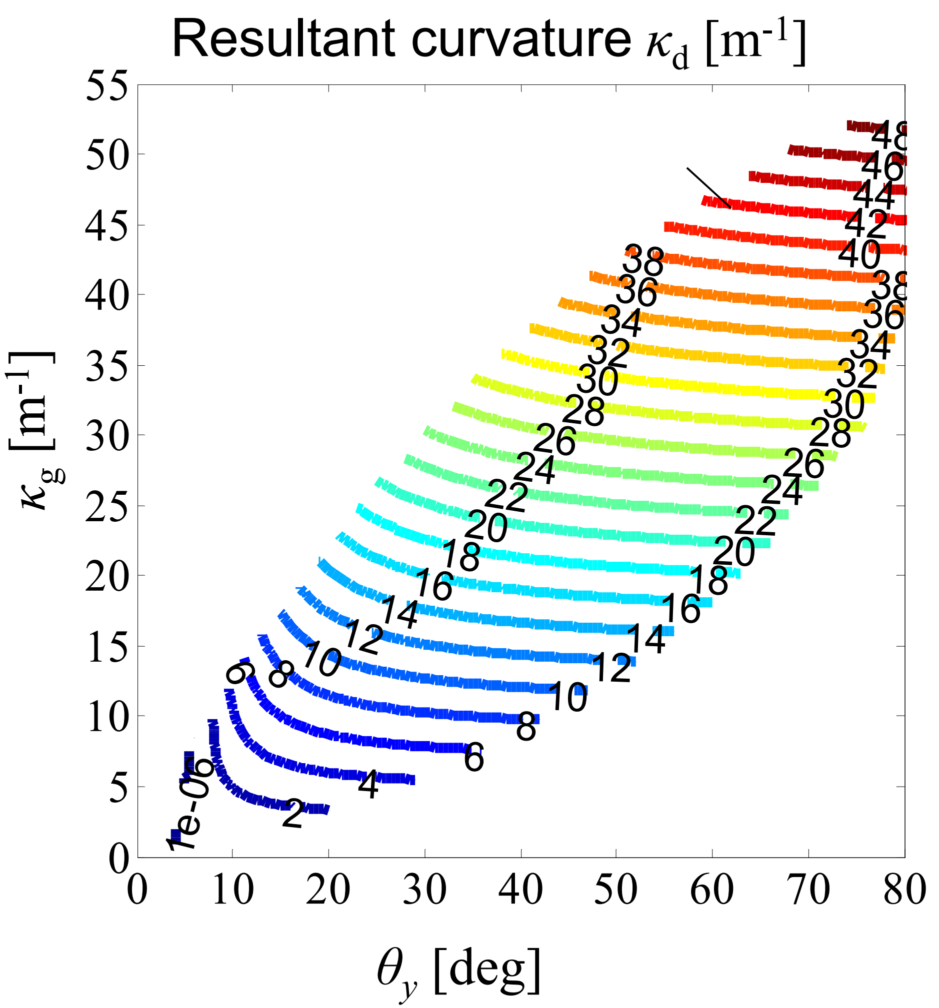

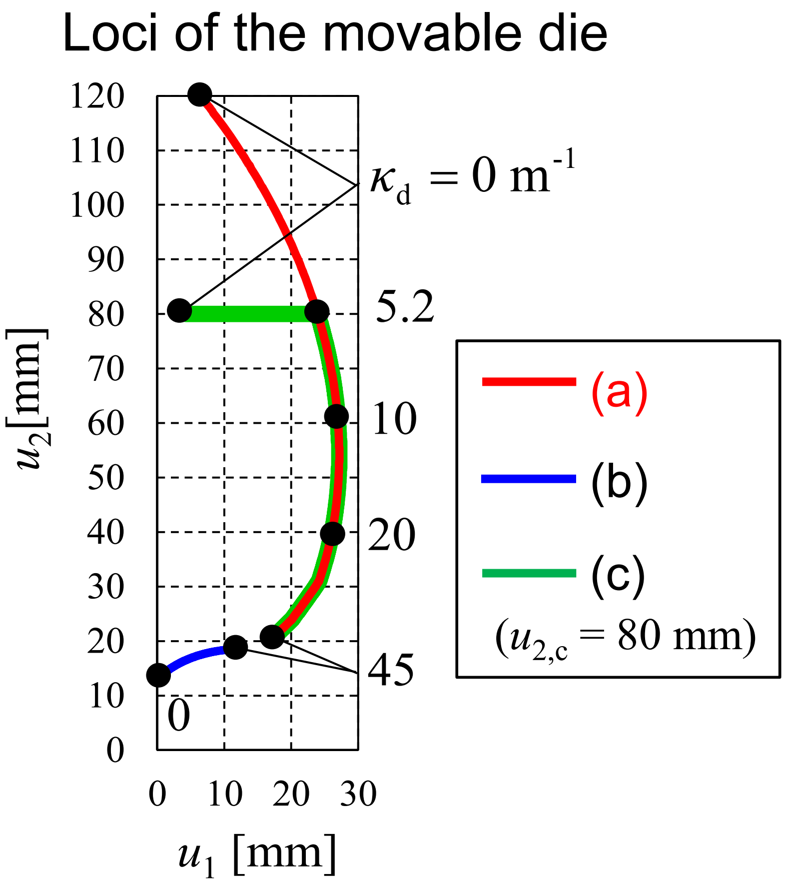

Effect of strategy (a): Reduction of the effect of positioning error on the result of bending

Results of calculation

Strategy for Determining Mov

it is also known that in strategy (a) due to the large change in the position of the movable die according to the target curvature, less effect of the positioning error of the movable die on the error of the bent pipe’s shape as well as the reduction of bending force shown in the left figure can be expected.

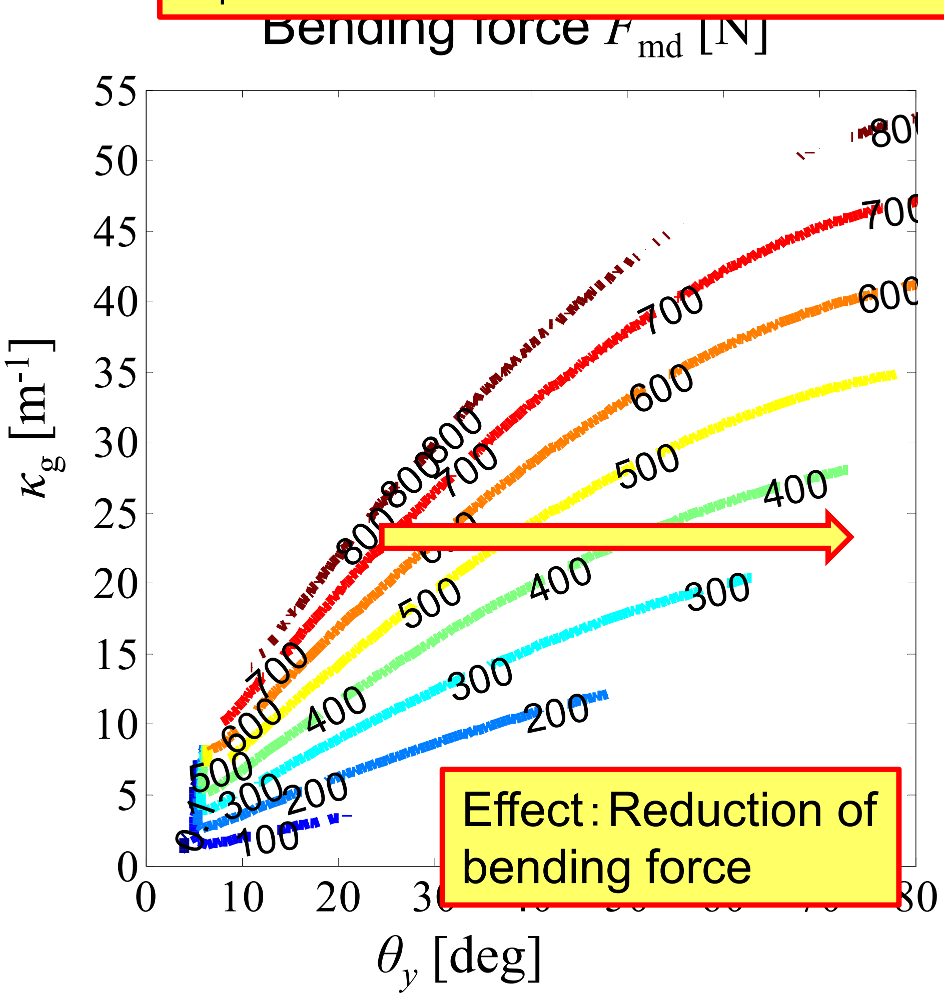

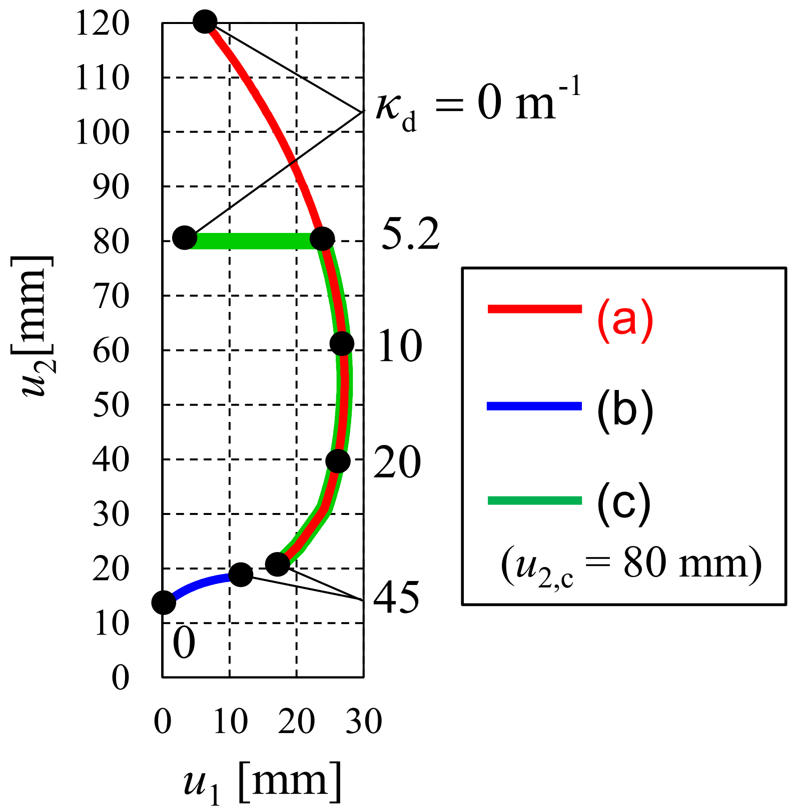

Effect of strategy (a): Reduction of the effect of positioning error on the result of bending

Results of calculation

Experiments

Measured radius R

After bending for a variety set of (R_g, θ_y)

Error

$$e = (R_d - R) / R$$

Estimated radius R_d

From the model as a function of (R_g, θ_y)

Result

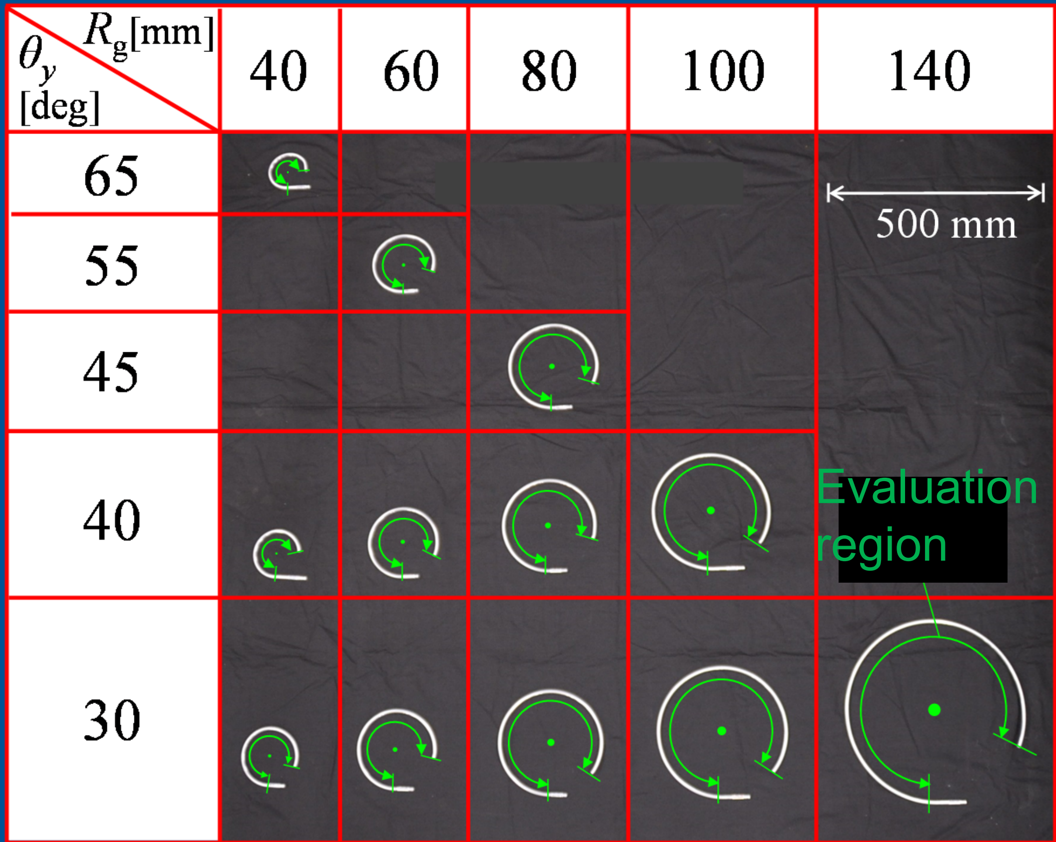

Experiments

It is known from the right figure that high estimation accuracy in the maximum tilt area was achieved (less than 2 %) though maximum error was 20%. These results agree with the theoretical results.

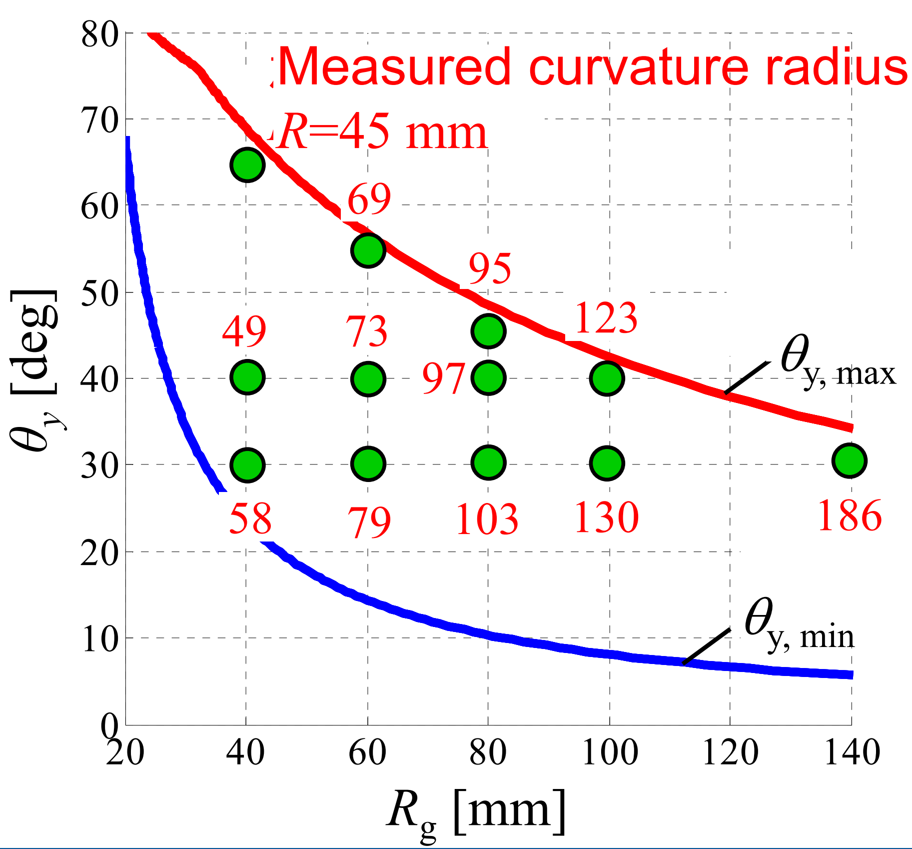

Measurement results

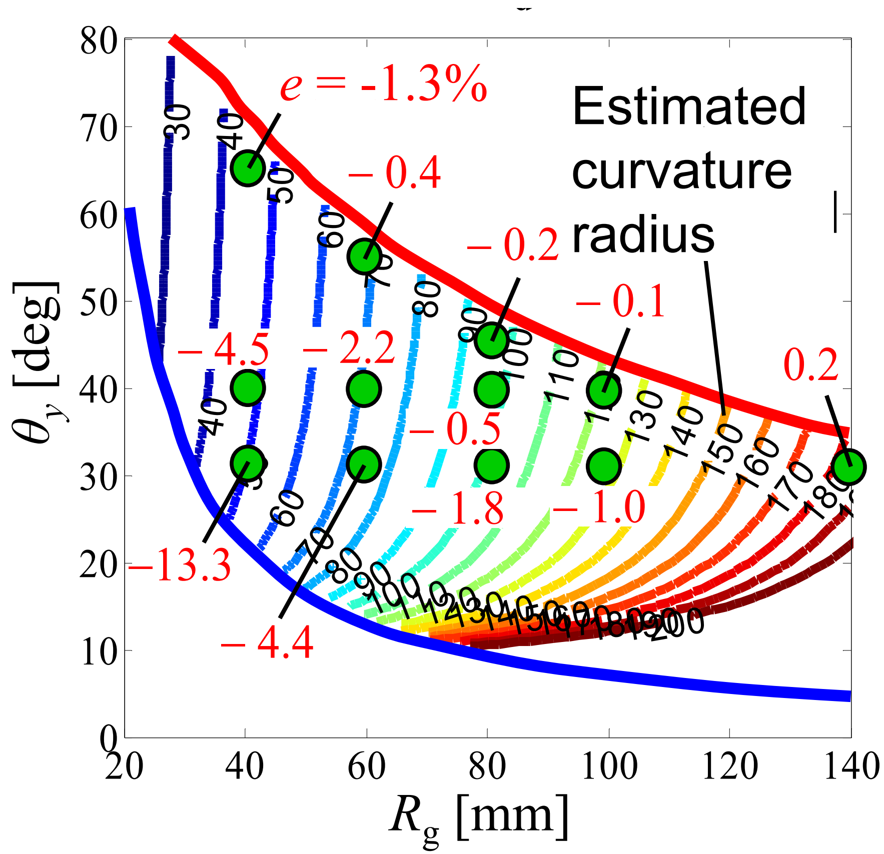

Estimated curvature radius and its error

Experiments

(Clothoid curve with variable curvature radius)

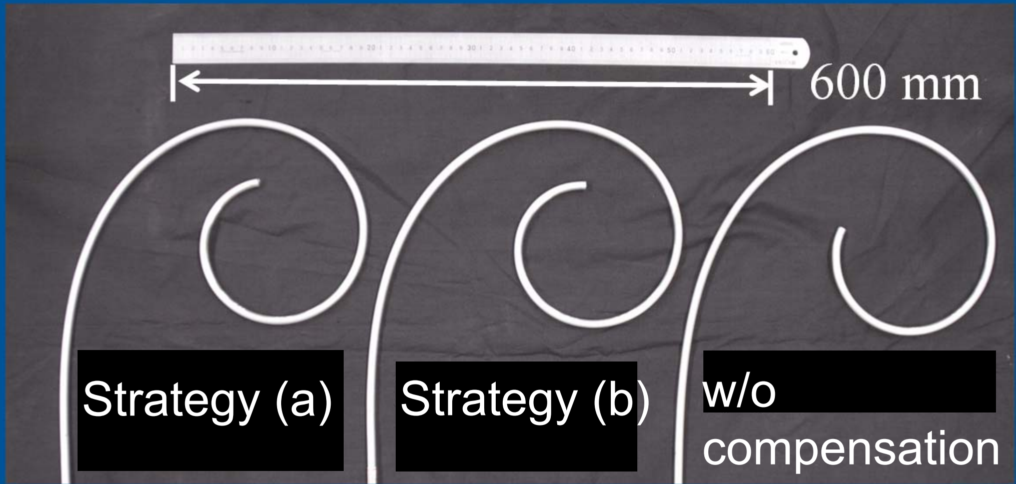

Result of bending

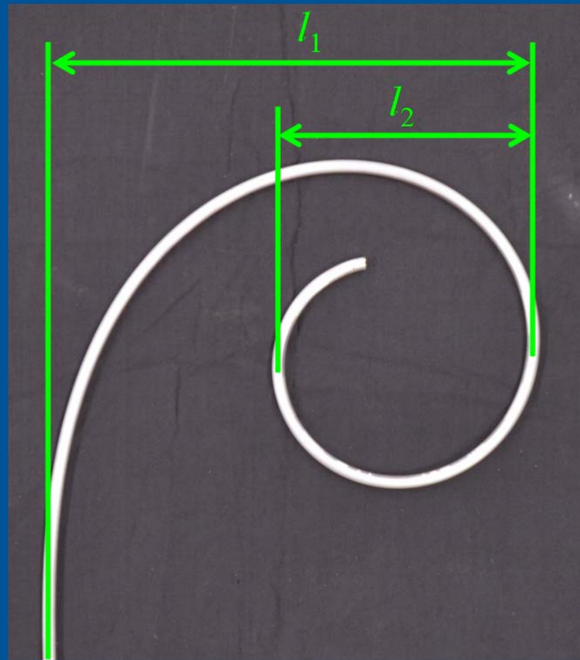

Measured values

Bending error

	Target shape	(a)	(b)	w/o compensation
l_1 [mm]	300.0	312	316	326
Error [%]	–	4.0	5.3	8.7
l_2 [mm]	158.6	160	160	164
Error [%]	–	0.9	0.9	3.4

Precise bending has been achieved by compensation based on the pose determination strategy using the maximum tilt angle.

Summary-Springback compensation

The conclusions are summarized as follows:

(1) A theoretical model to estimate the curvature of bent pipes in the penetration bending method has been developed by constructing a procedure to calculate the center line of the bent pipe from the pose of the movable die taking into consideration the effect of the springback of pipe and clearances at the dies.

(2) A bending strategy to perform precise bending, in which the pose of the movable die is determined so that the tilt of the movable die is maximized, has been proposed based on the maps of estimated curvature of bent pipe and bending force, which are obtained from the model in (1).

(3) Effectiveness of the proposed model and bending strategy has been validated through experiments by our prototype pipe bender using the 3-RPSR parallel mechanism.

Summary and Future Work

Results:

- ✓ Kinematic Design of Movable-Die Drive Mechanism with Orientation Capability which Enables Bending of Pipes with Complex Shapes
- ✓ Design of Movable-Die Drive Mechanism with High Stiffness to Achieve Precise Bending
- ✓ Modeling of penetration pipe bending and compensation of springback of pipe and clearance at dies
- ✓ Prototyping
- ✓ Experimental validation

Future Work:

- ✓ Development of pipe feeder enabling large feed force
- ✓ Precise pipe bending with 3D shape with shape and force feedback information

References

1. Kawasumi, S., et al, Precise Pipe-Bending by 3-RPSR parallel mechanism considering the effect of springback and dies clearances, Proceedings of 2014 Workshop on Fundamental Issues and Future Research Directions for Parallel Mechanisms and Manipulators, Jul. 2014.
2. M.-Mullio, M. et al, Kinematics and dynamics of a 3-RPSR parallel robot used as a pipe-bending machine, Advances in Robot Kinematics, Springer, pp. 307-316., Jun. 2014.
3. Takeda, Y., et al, Kinematic design of 3-RPSR parallel mechanism for movable-die drive mechanism of pipe bender, Romanian Journal of Technical Sciences Applied Mechanic, Vol. 58, No. 1-2, pp. 71-96, Mar. 2013.
4. Castillo-Castaneda, E., et al, Pose estimation of a six degrees of freedom pipe-bender using a 3D-visual measurement system of high accuracy, Proceedings of 3rd IFToMM International Symposium on Robotics and Mechatronics (ISRM2013), pp. 799-808, Oct. 2013.
5. Takeda, Y., et al, Kinematic analysis and design of 3-RPSR parallel mechanism with triple revolute joints on the base, International Journal of Automation Technology, Fuji Technology Press Ltd., Vol. 4, No. 4, pp. 346-354, Jul. 2010.
6. Takeda, Y., et al, Development of a pipe bender using a parallel mechanism with 3-RPSR structure with six degrees of freedom, Proceedings of 13th World congress in Mechanism and Machine Science, Jun. 2011.

Inverse displacement analysis

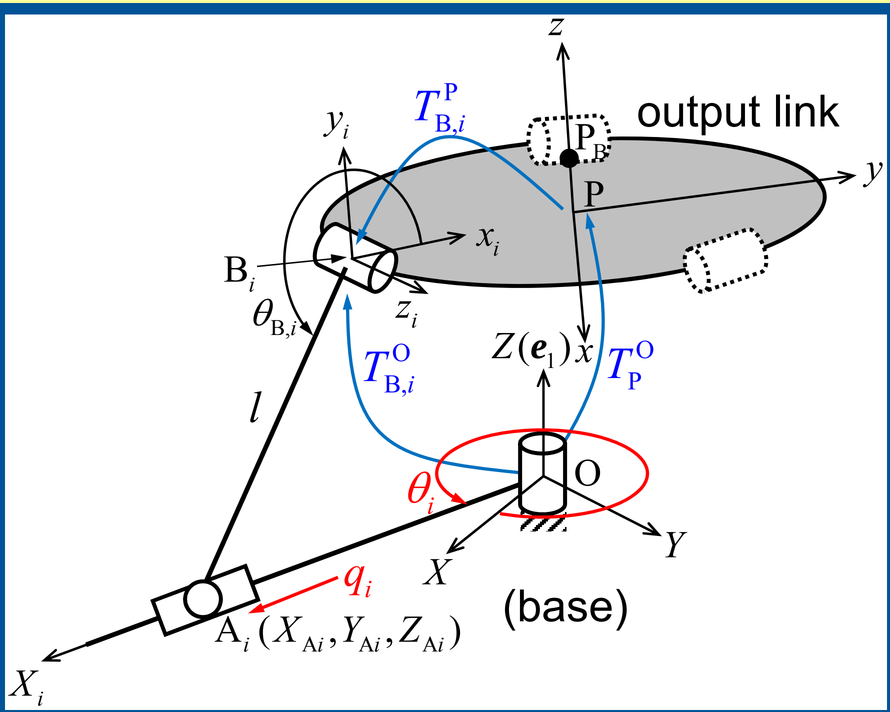

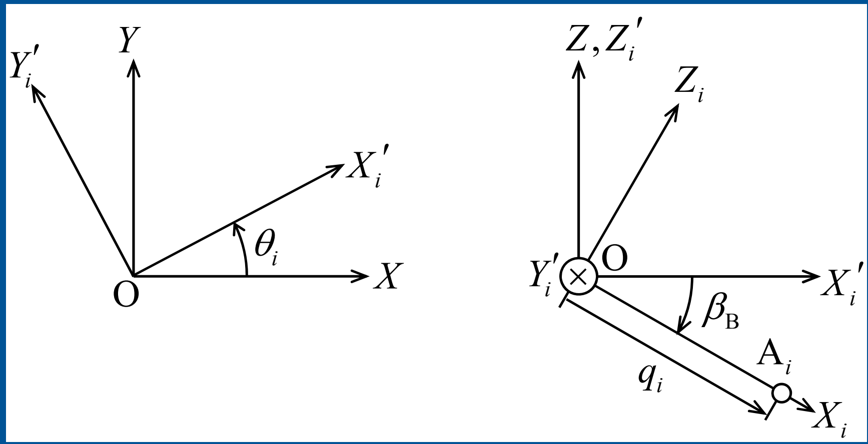

Definition of symbols

Quadratic equation in x_i and y_i:

$$x_i^2 + y_i^2 = l^2$$

$$\{(X_{\mathrm{B},i} + a_{11}x_i + a_{12}y_i)^2 + (Y_{\mathrm{B},i} + a_{21}x_i + a_{22}y_i)^2\}\tan^2\beta_{\mathrm{B}} = (Z_{\mathrm{B},i} + a_{31}x_i + a_{32}y_i)^2$$

Once the pose of the output link is given, the position and orientation of the coordinate system B_i-$x_i y_i z_i$ on the output link is obtained. Then, the position of A_i with respect to the coordinate system B_i-$x_i y_i z_i$ can be written as the circle centered on B_i and radius l. A_i moves on the circular cone defined by a point O, Z axis and angle β_{B}.

Inverse displacement analysis

Tokyo Institute of Technology
Mechanical Systems Design Lab.

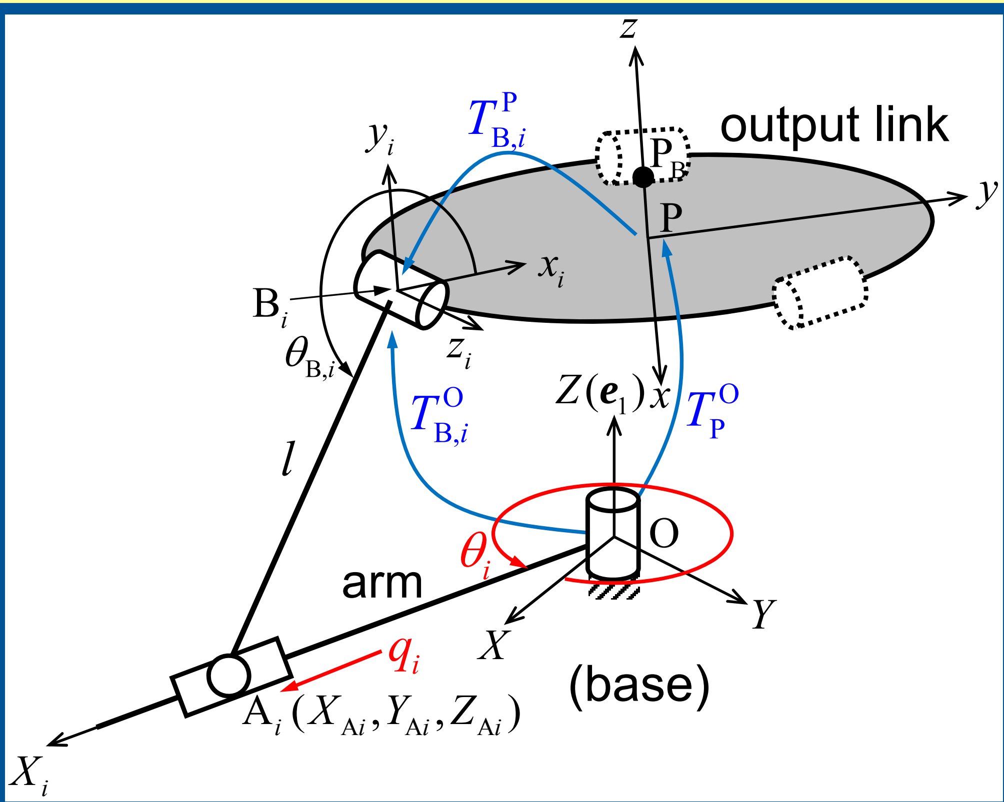

Definition of symbols

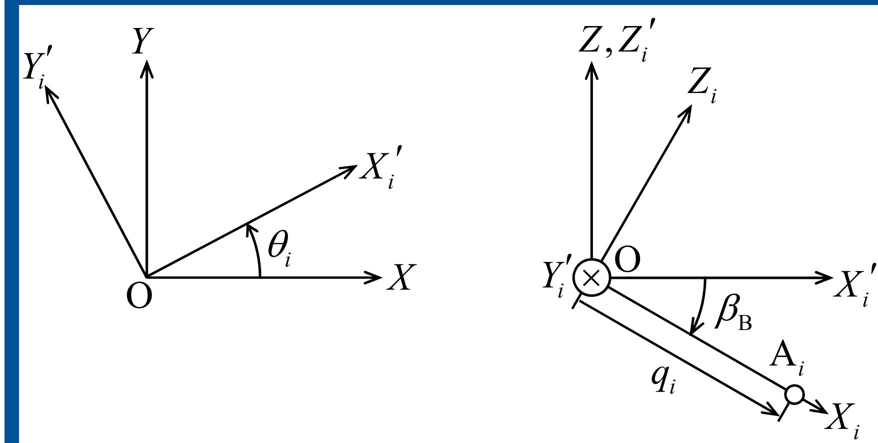

Definition of input displacements

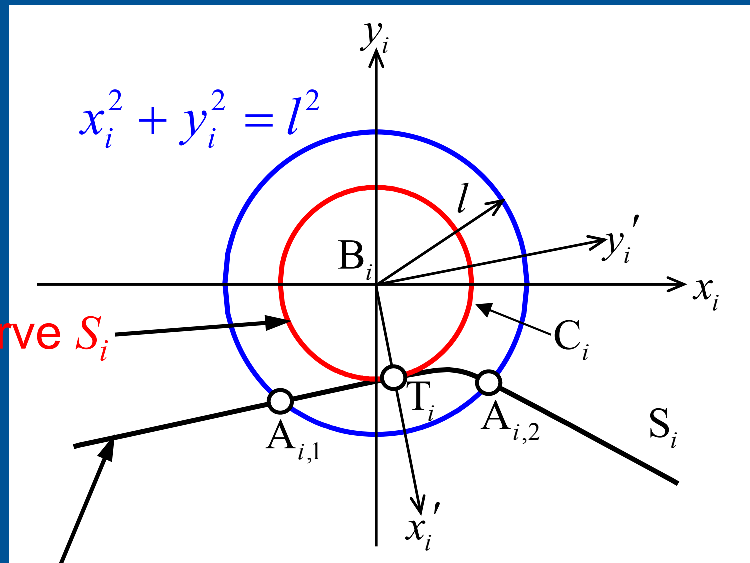

Tangential circle to curve S_i

Identification of the solution corresponding to the working mode from the two solutions by means of the y'-coordinate of A_i

$$\{(X_{\mathrm{B},i} + a_{11}x_i + a_{12}y_i)^2 + (Y_{\mathrm{B},i} + a_{21}x_i + a_{22}y_i)^2\}\tan^2\beta_{\mathrm{B}} = (Z_{\mathrm{B},i} + a_{31}x_i + a_{32}y_i)^2$$

Jacobian matrix

Tokyo Institute of Technology
Mechanical Systems Design Lab.

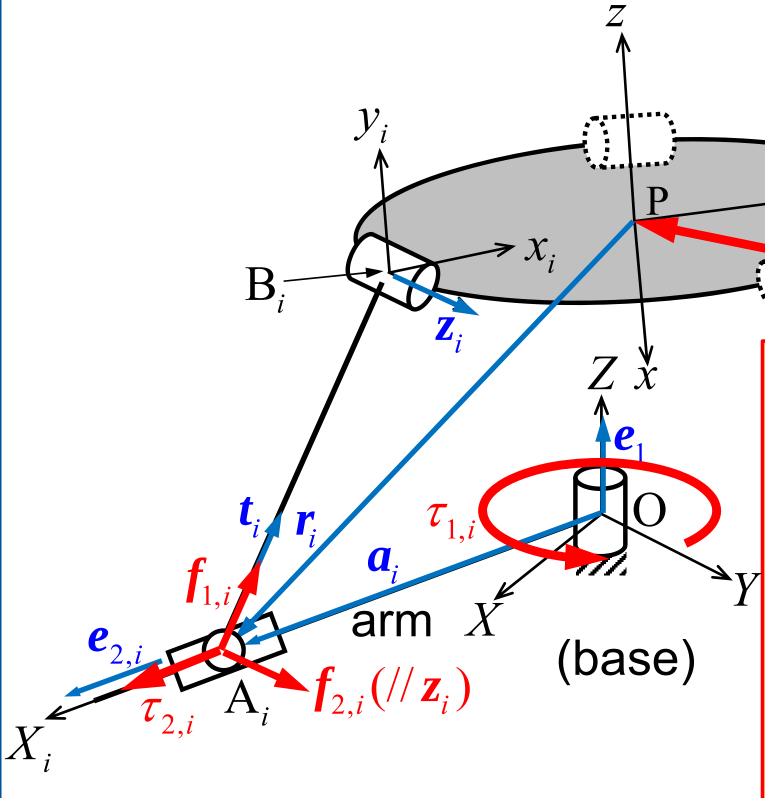

- $\tau_{1,i}$: input torque(R)
- $\tau_{2,i}$: input force(P)
- $\boldsymbol{F}$: external force
- $\boldsymbol{M}$: external moment
- $f_{1,i}$: joint force
- $f_{2,i}$: joint force

External force, input torque/force and joint forces

External force vs. input force/torque:

$$\begin{bmatrix} \boldsymbol{F} \\ \boldsymbol{M} \end{bmatrix} = -J_1 J_2^{-1} \begin{bmatrix} \boldsymbol{\tau}_1 \\ \boldsymbol{\tau}_2 \end{bmatrix} = -J\boldsymbol{\tau}$$

Equilibrium equation for force and moment w.r.t. output link:

$$\begin{bmatrix} \boldsymbol{F}^{\mathrm{O}} \\ \boldsymbol{M}^{\mathrm{O}} \end{bmatrix} = -J_1 \boldsymbol{f}$$

Relationship between joint forces and input force/torque:

$$\boldsymbol{\tau} = J_2 \boldsymbol{f}$$

Matrices J_1 and J_2:

$$J_1 = \begin{bmatrix} \mathbf{t}_1 & \mathbf{t}_2 & \mathbf{t}_3 & \mathbf{z}_1 & \mathbf{z}_2 & \mathbf{z}_3 \\ \mathbf{r}_1 \times \mathbf{t}_1 & \mathbf{r}_2 \times \mathbf{t}_2 & \mathbf{r}_3 \times \mathbf{t}_3 & \mathbf{r}_1 \times \mathbf{z}_1 & \mathbf{r}_2 \times \mathbf{z}_2 & \mathbf{r}_3 \times \mathbf{z}_3 \end{bmatrix}$$

$$J_2 = \begin{bmatrix} \{\boldsymbol{a}_1 \times \boldsymbol{t}_1, \boldsymbol{e}_1\} & 0 & 0 & \{\boldsymbol{a}_1 \times \boldsymbol{z}_1, \boldsymbol{e}_1\} & 0 & 0 \\ 0 & \{\boldsymbol{a}_2 \times \boldsymbol{t}_2, \boldsymbol{e}_1\} & 0 & 0 & \{\boldsymbol{a}_2 \times \boldsymbol{z}_2, \boldsymbol{e}_1\} & 0 \\ 0 & 0 & \{\boldsymbol{a}_3 \times \boldsymbol{t}_3, \boldsymbol{e}_1\} & 0 & 0 & \{\boldsymbol{a}_3 \times \boldsymbol{z}_3, \boldsymbol{e}_1\} \\ \{\boldsymbol{t}_1, \boldsymbol{e}_{2,1}\} & 0 & 0 & \{\boldsymbol{z}_1, \boldsymbol{e}_{2,1}\} & 0 & 0 \\ 0 & \{\boldsymbol{t}_2, \boldsymbol{e}_{2,2}\} & 0 & 0 & \{\boldsymbol{z}_2, \boldsymbol{e}_{2,2}\} & 0 \\ 0 & 0 & \{\boldsymbol{t}_3, \boldsymbol{e}_{2,3}\} & 0 & 0 & \{\boldsymbol{z}_3, \boldsymbol{e}_{2,3}\} \end{bmatrix}$$

Singular configuration

Tokyo Institute of Technology
Mechanical Systems Design Lab.

(a) Uncertain configuration: At this configuration, the matrix J_1 loses its full rank. Typical configurations are (a-1) axes of revolute joints on the output link z_i and points A_i of two connecting chains are located in a plane, (a-2) points A_i of two connecting chains coincide: Physically unavailable due to collision of two arms.

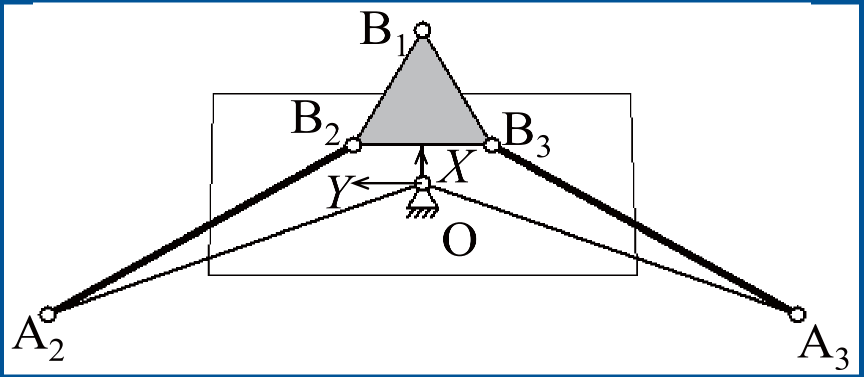

Example of uncertain configuration(a-2)

(b) Stationary configuration: At this configuration, the matrix J_2 loses its rank. This configuration occurs when the curve S_i is tangent to the circle of radius l (solution of inverse displacement analysis).

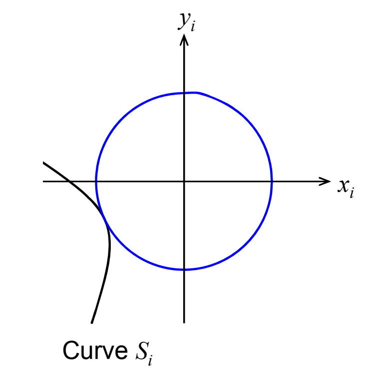

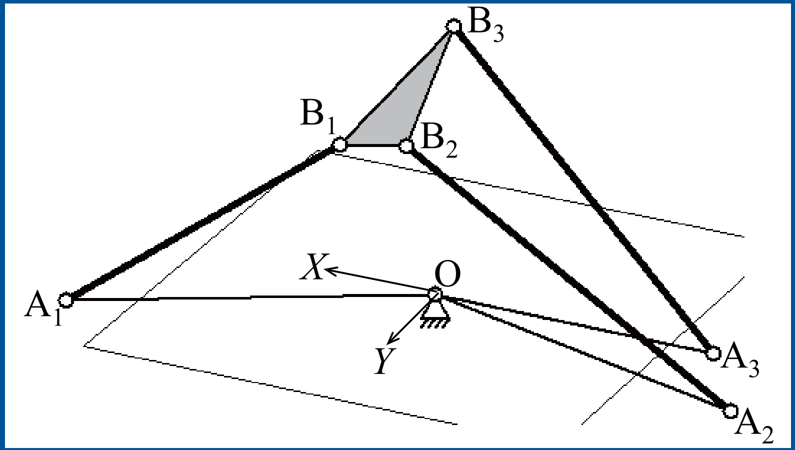

Example of stationary configuration(b)

$$\begin{bmatrix} \boldsymbol{F} \\ \boldsymbol{M} \end{bmatrix} = -J_1 J_2^{-1} \begin{bmatrix} \boldsymbol{\tau}_1 \\ \boldsymbol{\tau}_2 \end{bmatrix} = -J\boldsymbol{\tau}$$

Conclusions and future work

Tokyo Institute of Technology
Mechanical Systems Design Lab.

Kinematic analysis of a 3-RPSR parallel mechanism with six DOF, which has been applied to a movable-die drive mechanism of pipe bender, has been done to clarify the relationship between its design parameters and orientation capability. Based on the results of analysis, a mechanism that can achieve a high orientation capability was designed, and a prototype has been built. Its orientation capability has been revealed, and it has been shown that our prototype mechanism achieved a superior orientation capability.

Future work includes

- evaluation of accuracy, stiffness
- evaluation of pipe-bending performance
- ect.